

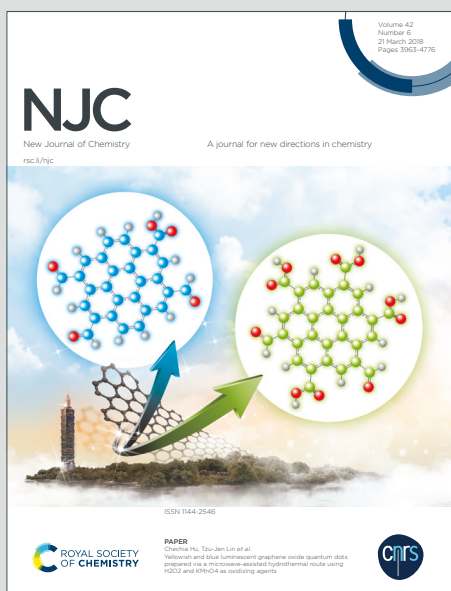
NJC

New Journal of Chemistry

Accepted Manuscript

A journal for new directions in chemistry

This article can be cited before page numbers have been issued, to do this please use: P. Ghosh and S. Santra, *New J. Chem.*, 2020, DOI: 10.1039/D0NJ00353K.



This is an Accepted Manuscript, which has been through the Royal Society of Chemistry peer review process and has been accepted for publication.

Accepted Manuscripts are published online shortly after acceptance, before technical editing, formatting and proof reading. Using this free service, authors can make their results available to the community, in citable form, before we publish the edited article. We will replace this Accepted Manuscript with the edited and formatted Advance Article as soon as it is available.

You can find more information about Accepted Manuscripts in the [Information for Authors](#).

Please note that technical editing may introduce minor changes to the text and/or graphics, which may alter content. The journal's standard [Terms & Conditions](#) and the [Ethical guidelines](#) still apply. In no event shall the Royal Society of Chemistry be held responsible for any errors or omissions in this Accepted Manuscript or any consequences arising from the use of any information it contains.

Fluorophoric [2]Rotaxanes: Post-Synthetic Functionalization, Conformational Fluxionality and Metal Ion Chelation

Saikat Santra^{a,b}, Pradyut Ghosh^{a*}

^a School of Chemical Science, Indian Association for the Cultivation of Science, Jadavpur, Kolkata 700032, India. Email. Id.: icpg@iacs.res.in

^b Department of Chemistry, Taki Government College, Taki, North 24 Parganas, West Bengal, India, Pin Code No. 743429.

Abstract

Herein, we report an amino-ether fluorophoric macrocyclic wheel (MC) based multi-functional [2]rotaxane. The said rotaxane is further functionalised to three different analogues as ROTa-c upon appending three different amide groups [-NC(O)R, where R = -CH₃, 4-fluorophenyl and tertiary butyl respectively]. Such post-synthetically analogues are characterised via mass spectrometry, 1D/2D NMR and optical spectroscopy. Steric effects exerted by the tertiary amide groups on the rotamer induced dynamic motions among ROTa-c are investigated via variable temperature NMR spectroscopy. Although the tri-acetylated ROTa and tri-aryl substituted ROTb show rotamer induced conformational/co-conformational diversities, one conformer is predominant in ROTc under identical experimental conditions due to the restricted rotation of bulky tertiary butyl groups. Interestingly, intramolecular exciplex formation between the wheel and the axle is exhibited by ROTa-c, which is established through detail emission studies in solution state. The exciplex emission generated by rotaxanes is monitored to predict the preferential coordination sites of metal ions (alkali and transition) in the above interlocked systems. Finally, chelating property of fluorophoric rotaxanes is investigated with different transition metal ions by absorption as well as emission spectroscopy studies.

Introduction

Mechanically Interlocked Molecules (MIM's) are the species in which more than one sub-component are generally entwined and held together without any direct covalent interactions but the sub components are unable to pass through one another. One of such MIM's is rotaxane which consist of a macrocyclic ring wrapped around a linear rod shaped axle.¹⁻⁴ Till date, significant progresses have been made for the development of MIM's using different templating agents like cations,⁵ anions^{1,6}, aromatic stacking interactions,⁷ H-Bonds,⁸ halogen bonds,⁹ chalcogen bonds^{10 a} etc. ^{10 b-d} Now a day, the exploration of MIM's including rotaxanes are increased dramatically for variety of applications such as sensing,¹ recognition,^{2,3} catalyst⁴, development of molecular machines etc. ¹¹⁻⁴⁸ One of such application is the

metal ion binding studies where the chelation occurs through endotopic manner in rotaxanes. Such endohedral binding is predictable but the coordination may change the conformation and significantly change their properties.^{48(a)}

On the other side, tertiary amide bond is popular to generate a set of rotamers *via* rotation around N-C(O) bond.⁴⁹ Based on this concept, Clayden and others have synthesized smart non-interlocked molecules as molecular gears upon introducing tertiary amide in the molecular frame work.^{28,50-53} However, the effect of such N-C(O) bond rotation of the tertiary amides embedded with the MIM's are studied rarely.^{54,55} Additionally, chemists are attracted to combine the electronic, chelating properties of metal ions⁵⁶⁻⁶⁰ with the photo-physical properties of MIMs in multiple ways.⁶¹⁻⁶⁶ Such property is useful to sense or recognize a guest and to promote/ regulate molecular motions.^{63,64} Intramolecular exciplex formation between the non-covalently attached molecules are one kind of examples of aforesaid phenomena. "Rotaxane exciplexes" are investigated by Swager *et al.* and their fundamental studies of supramolecular photochemistry are relevant to develop (i) new compounds with various photochemical/photophysical properties and (ii) chemical sensors.^{48(b)} In our recently published reports, we have demonstrated that tri-acetylated ring components of multi-functional [2]rotaxanes show rotamers induced dynamic property at room temperature, which can be controlled by the addition and removal of alkali metal ions.^{67,68} To reveal the cause of such controllable dynamic properties and effect of steric crowding at N-C(O) bond, herein, we report heteroditopic fluorophoric macrocyclic wheel based various tertiary amides appended [2]rotaxanes to explore (i) structure-property relationship in terms of rotamers induced conformational/ co-conformational variation, (ii) mechanistic details of the alkali metal ion triggered conformational/co-conformational changes, and (iii) transition metal ion binding properties of interlocked species by absorption and emission spectroscopic studies.

Results and Discussion

Designing aspects and strategies: *Designing aspects and strategies:* The targeted fluorophoric [2]rotaxanes and their non-interlocked components are depicted in **Chart 1**. The component of the rotaxanes integrates a naphthyl unit, which is strategically positioned opposite to the tris-amide pocket. In this respect, our previous result demonstrate that rotaxane show various conformations/ co-conformations upon tri acetylation.⁶⁷ The existence of different conformation/ co-conformation is due to the rotation around N-C(O) bonds in tertiary amides which are appended in the interlocked system (**Chart 1**). To investigate the steric effect on such conformations/ co-conformations, we have synthesized tertiary amide group functionalized new fluorophoric rotaxanes upon appending aryl rings and tertiary butyl groups along with acetyl group to rotaxanes composed of naphthyl integrated macrocyclic wheel (**Scheme 1 and 2**).

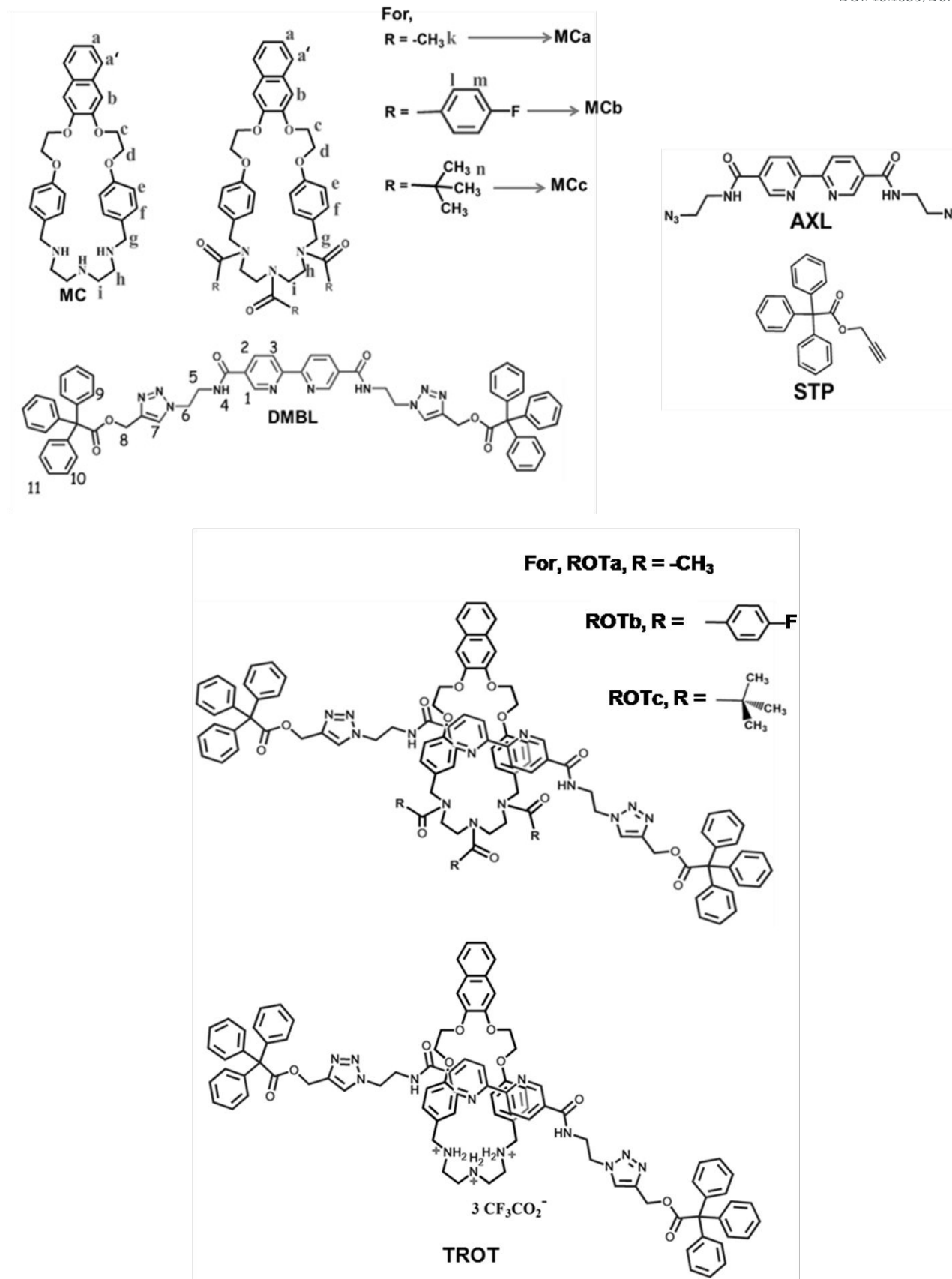
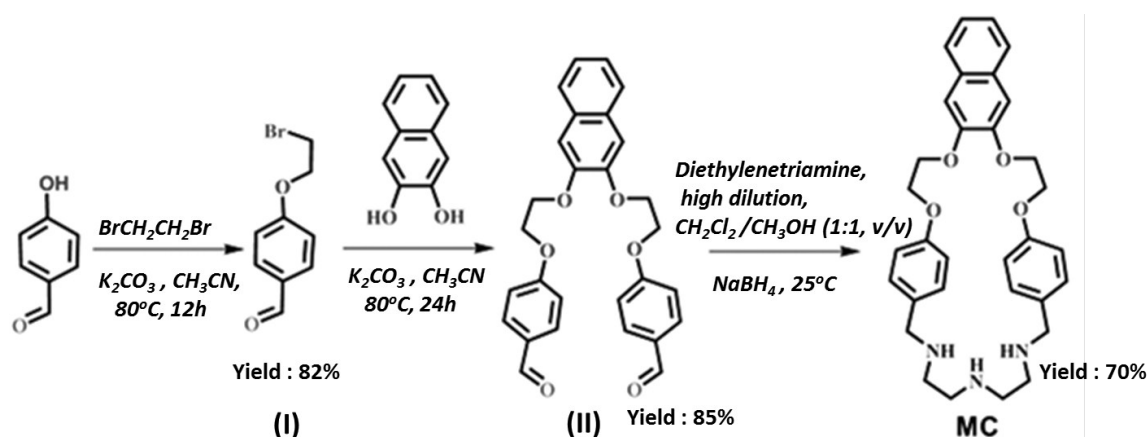


Chart 1. Chemical diagram of tertiary amide appended [2]rotaxanes ROTa-c, TROT and the non-interlocked components: MC, MCa-c, AXL, STP and DMBL with labelling (wherever necessary)

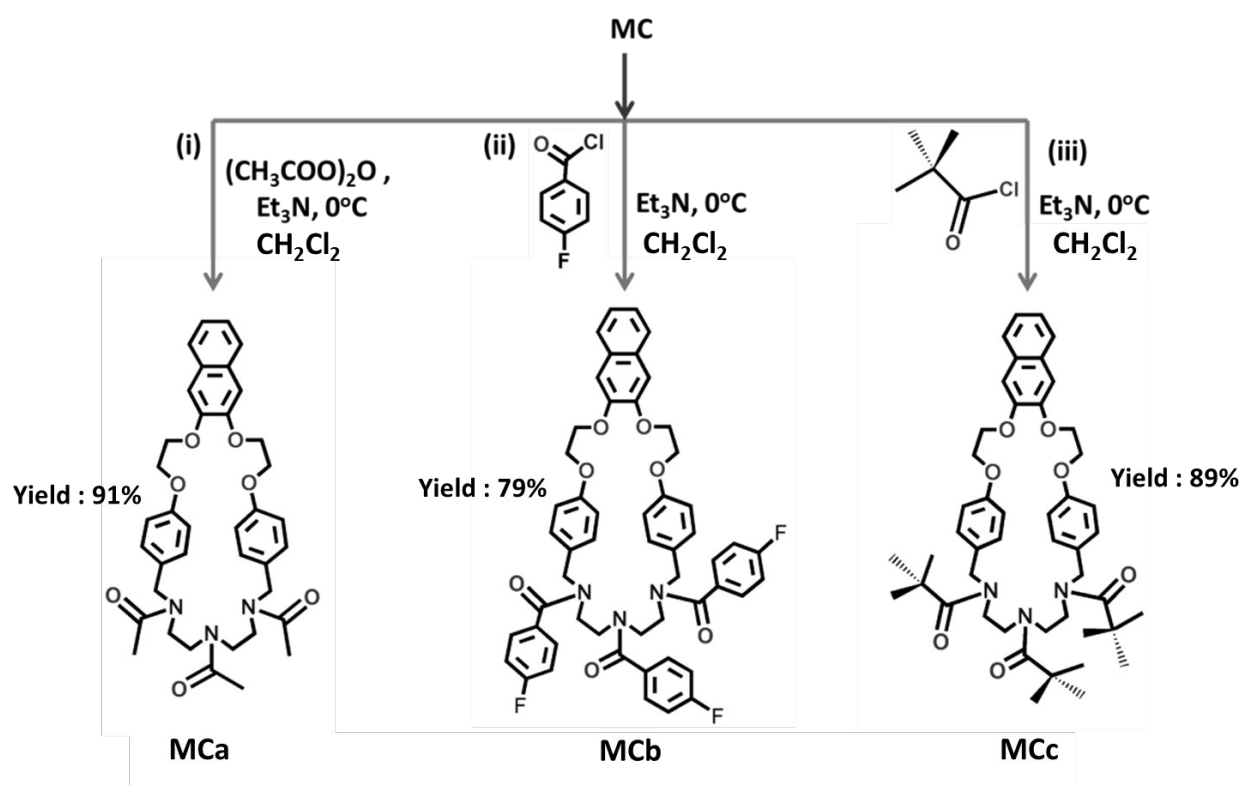
Thus such modifications would be useful to establish the structure-property relationships of rotamers induced dynamic property in multi-functional [2]rotaxanes and to confirm the actual binding site of metal ions during metal ion assisted conformational locking via detailed absorption and emission spectroscopic studies.

Synthesis of Interlocked Species: The new fluorophoric macrocycle (MC) and their derivatives (MCa-c) are synthesised using high dilution method as described in the experimental section (*Scheme 1*).

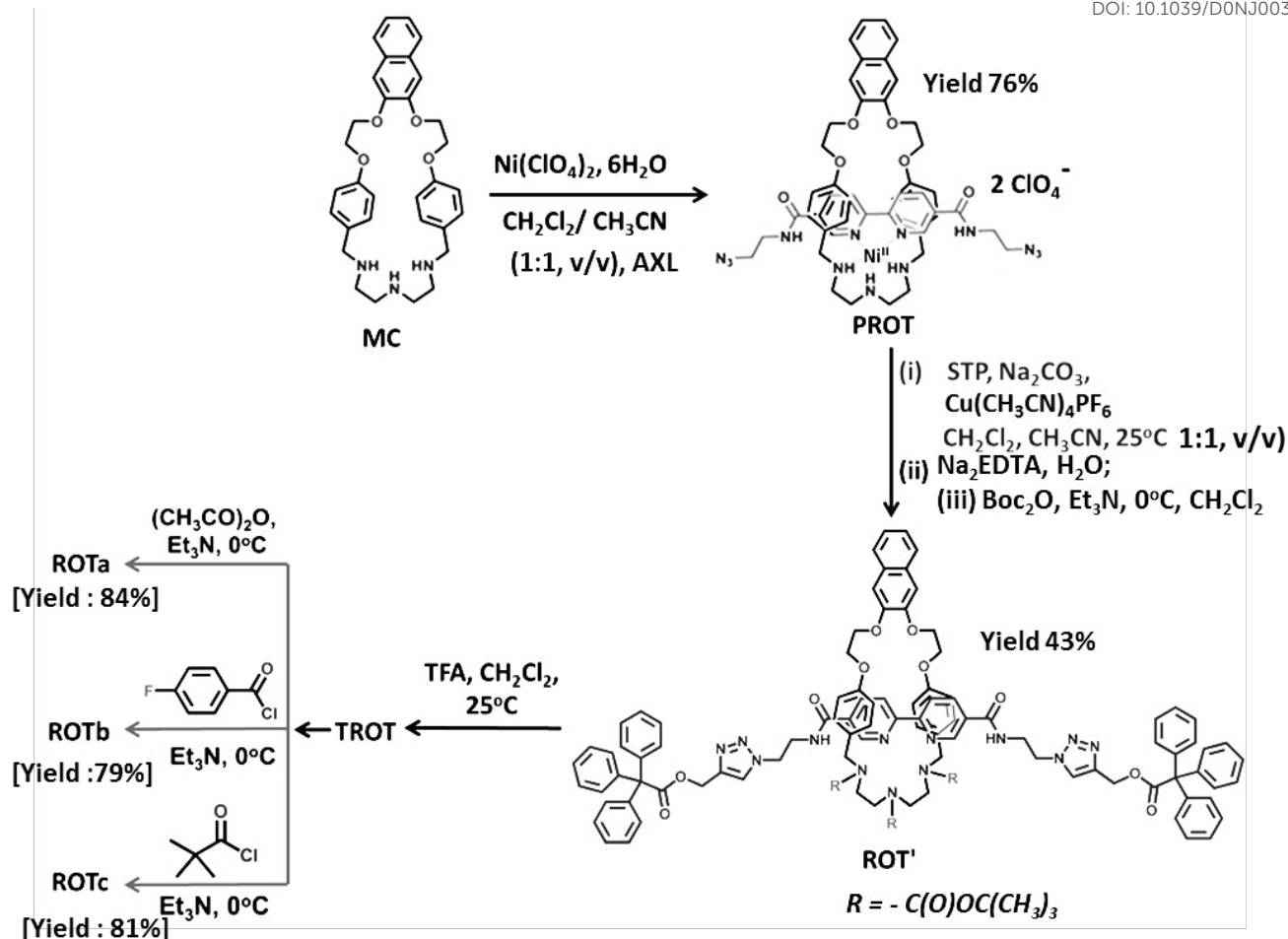
[A]



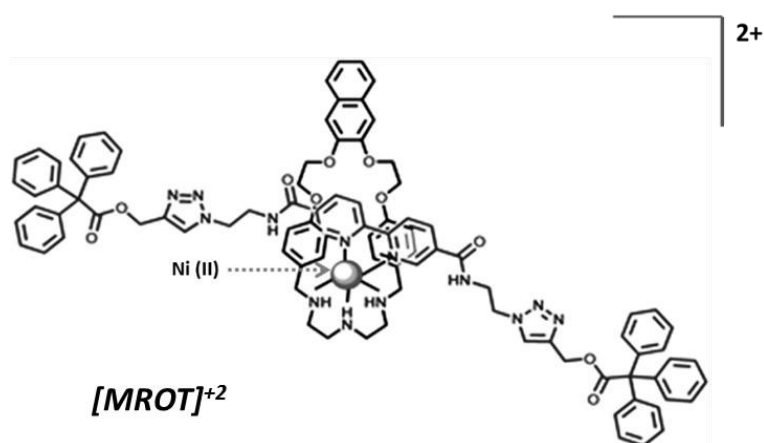
[B]



Scheme 1 [A] Synthetic route of macrocycle MC (Yield: 70 %). [B] Synthetic route of the functionalised macrocycles MCa-c.



[Chemical Diagram of AXL and STP are shown in Chart 1]



Scheme 2. Synthetic route of Ni^{II} templated [2]pseudorotaxane, (PROT) (Yield : 76%); synthetic route of ROT' [Yield: 39%] where R = -C(O)OC(CH₃)₃; de-protected ROT' and synthetic route of functionalized [2]rotaxanes, ROTa-c within 79% to 82 % yield from [TROT]. Chemical diagram of [MROT]²⁺. Chemical diagram of [TROT] and ROTa-c, are depicted in Chart 1. [Boc₂O = Di-tertiary-butyl dicarbonate].

Characterization spectra of MC, MCa-c and their precursors are depicted in *Figure 1S - 23S* in ESI†. It is to be noted that absorption spectra of MCa-c show peaks at the region of 212 - 300 nm whereas upon excitations of MCa-c at 285 nm, result in luminescence spectrum at ~340 nm in 9:1 (v/v) CH₃CN/CHCl₃ solvent mixture (*Figure 23S* in ESI†). Then the fluorophoric wheel, MC is employed to synthesise rotaxanes via passive metal ion templation method. The reaction of MC with Ni^{II} and azide terminated axle, AXL forms MC based [2]pseudorotaxane, PROT (*Scheme 2, Chart 1* and *Figure 24S-28S* in ESI†). PROT and alkyne-terminated stopper, STP are used as precursors to generate metallated [2]rotaxane, MROT via click reaction (*Chart 1, Scheme 2, Figure 29S* in ESI†).

From MROT, three functionalised [2]rotaxanes (ROTa-c) are synthesized as post synthetic functionalization ROT' and isolated in good yields in the range of 79-82% (*Scheme 2*). Successful formation of tris tertiary amide functionalised rotaxanes are evidenced by mass spectrometry, ¹H-NMR, ¹³C NMR, COSY, NOESY, ROESY, DOSY spectroscopy, MALDI mass spectrometry and optical spectroscopic studies. Detailed synthesis, characterization and electronic spectral data are described in experimental section. Characterization spectra are given in ESI† section (*Figure 30S - 71S* in ESI†).

Comparative NMR spectra of the post-synthetically functionalised rotaxane and their non-interlocked subcomponents: The conjoint shielding effect among aromatic π systems due to the donor-acceptor interactions is clearly evident upon interlocking, from the comparative ¹H-NMR spectrum of interlocked species and those of its non-interlocked counterparts. A comparison of the ¹H NMR spectrum of rotaxane (ROTa-c) with those of its non-interlocked components, MCa-c and axle (DMBL) in DMSO-d₆ reveals significant upfield shifts in the signals for the two lateral aromatic macrocycle protons Ar-H^e and Ar-H^f and bipyridine protons Ar-H^{1,2,3} upon interpenetration (*Figure 1*).

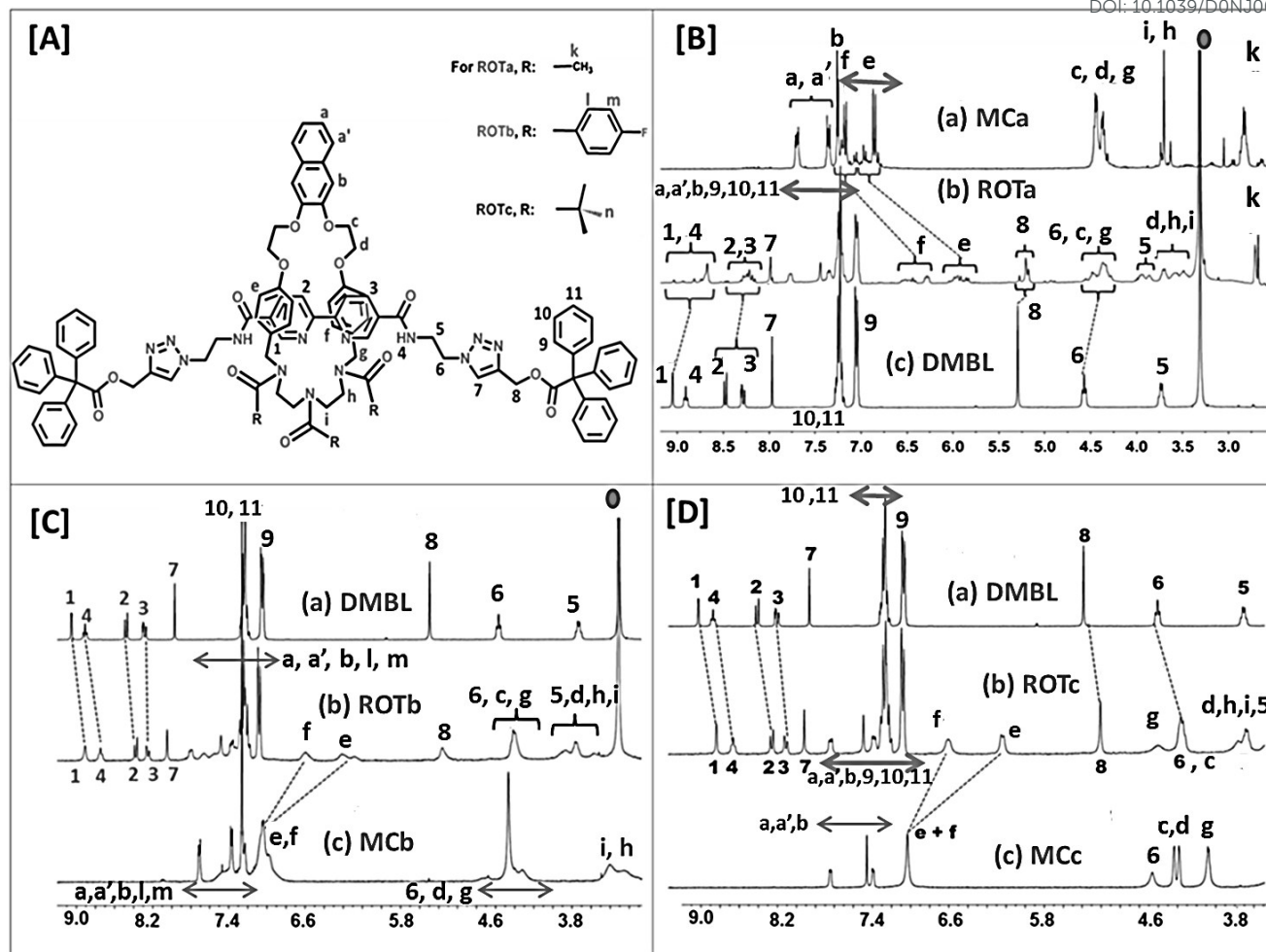
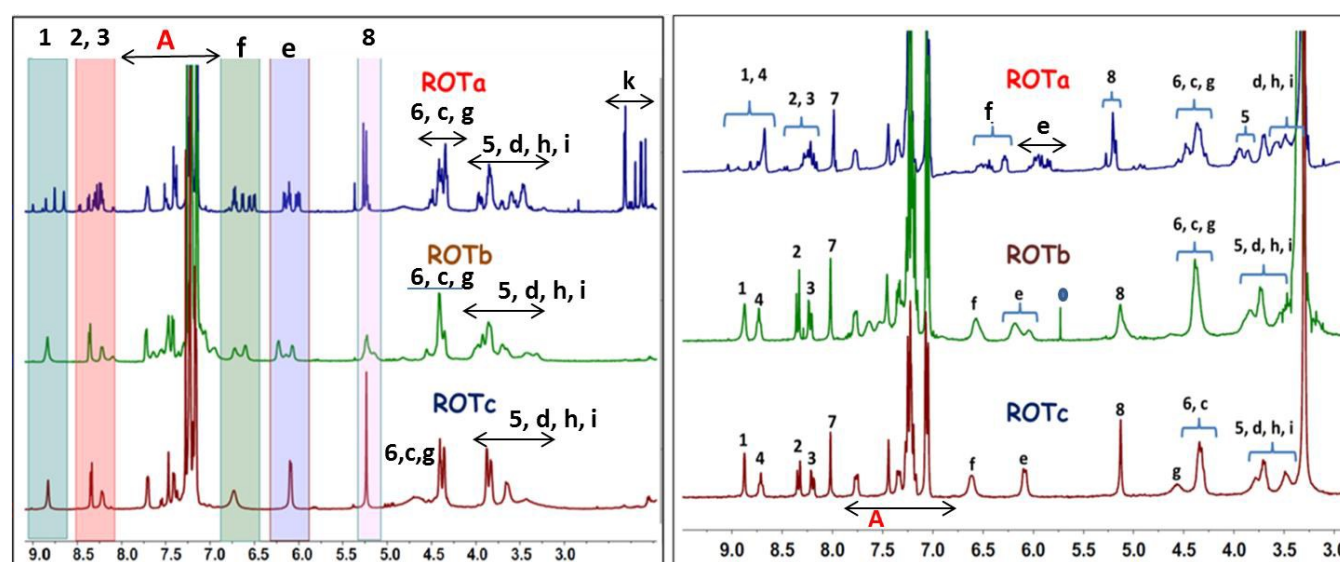
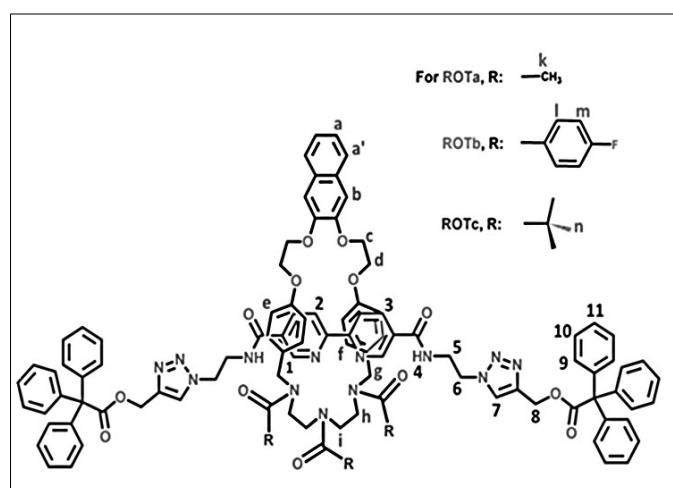


Figure 1. [A] Chemical diagram of functionalised Rotaxanes **ROTA-c** with labels. [B] Comparative $^1\text{H-NMR}$ spectra of (a) **MCA**, (b) **ROTA**, (c) Centre piece **DMBL**; [C] Comparative $^1\text{H-NMR}$ spectra of (a) **DMBL**, (b) **ROTB**, and (c) **MCb**; [D] Comparative $^1\text{H-NMR}$ spectra of (a) **DMBL**, (b) **ROTC**, and (c) **MCC**. All the studies are carried out in DMSO-d_6 solvent at 298 K (300 MHz). The circle marked proton ($\delta = 3.46$ ppm) indicate the solvent. Labelling corresponds to the proton signals which are mentioned in the chemical diagram of Chart 1.

It is mentioned in the introduction section that tertiary amides are capable to generate rotational isomers due to rotation around N-C(O) bonds.^{28,49} Since the post-synthetically functionalised rotaxanes **ROTA-c** composed of various tertiary amide moieties, it is expected that they will show existence of different rotational isomers in solution and indeed the $^1\text{H-NMR}$ spectra of most of the rotaxane (**ROTA-b**) show the peak multiplicities due to the existence of various rotational isomers. Comparative analyses of the $^1\text{H-NMR}$ spectra of the functionalized rotaxanes show that with respect to the tri-acetyl substituted rotaxane (**ROTA**), the peak multiplicities in aryl substituted rotaxane (**ROTB**) is notably decreased (**Figure 2**). These observations clearly indicate that due to the restricted rotation of aryl ring compared to the acetyl group appended rotaxanes, numbers of conformers and co-conformers are less in **ROTB** as

compared to ROTa under identical conditions in both CDCl_3 and in DMSO-d_6 solvent. On the other side, $^1\text{H-NMR}$ spectrum of ROTc shows the absence of peak multiplicity/ broadening that indicates the preference of a single conformer/ co-conformer over other under identical experimental conditions. We have also carried out low temperature $^1\text{H-NMR}$ of ROTb and ROTc in CDCl_3 which show that our assumptions are quite precise, as the preferential existence of one conformer of ROTc is noticed upto 243 K (Figure 63S - 64S in ESI †). As the size of tertiary butyl group is larger, the three bulky group in ROTc may not allow to rotate freely the tertiary $-\text{NC}(\text{O})$ bond in ROTc. But such rotations are comparatively facile in ROTa due to the small size of acetamido group and as a consequence of that multiple conformers/ co-conformers exist in ROTa and comparatively less numbers of rotational isomers are exist in ROTb and in ROTc.



“A” marked zone ($\delta = 7.0 - 7.8$ ppm) represents the proton signals corresponds to a, a', b, 9, 10, 11 for ROTa and ROTc whereas, for ROTb: a, a', b, l, m, 9, 10, 11 marked protons represent the A zone

Figure 2. Comparative $^1\text{H-NMR}$ spectra of ROTa (Top), ROTb (Middle), and ROTc (Bottom) at 298 K (300 MHz) in CDCl_3 (left) and in DMSO-d_6 (right). The blue circle in the spectrum of ROTb in right

indicates the peak ($\delta = 5.76$ ppm) corresponds to dichloromethane solvent impurity. The labels of the protons are depicted in the chemical diagram of the [2]rotaxanes (Top).

Rotamer induced conformational fluxionality studies via variable temperature $^1\text{H-NMR}$:

VT- $^1\text{H-NMR}$ spectroscopy are carried out in cases of all the substituted rotaxanes to imply the transition from slow state to the time average state (Figure 60S, 61S and 62S for ROTa and ROTc respectively in ESI†, Figure 3 for ROTb).

ROTa: Multiplicity in case of ROTa resembles our previously published report.^{67, 68} $^1\text{H-NMR}$ spectral evidences from Figure 60S in ESI† shows that aromatic protons of the bipyridine part of the centre piece, H_{Ar}^1 , H_{Ar}^2 and H_{Ar}^3 which resonates at $\delta = 8.62$ to 8.74 and 8.15 to 8.30 ppm as multiplets, start to accumulate with increasing temperature and finally coalesce at 370 K. With increasing temperature, amide $-\text{NH}^4$ protons show gradual upfield shift due to the cleavage of intermolecular H-bond with the polar solvent (DMSO- d_6). At 370 K, $-\text{NH}^4$ merged with the proton signals appeared for H_{Ar}^2 and H_{Ar}^3 with proper integral value. Proton signals associated with the wheel component of ROTa shows peaks multiplicity at $\delta = 6.25$ to 6.73 ppm and $\delta = 5.70$ to 6.09 ppm for H_{Ar}^f and H_{Ar}^e respectively, they started to accumulate with increasing temperature and finally coalesce into two different set of peaks at 6.03 and 6.48 ppm with proper integration ratio at high temperature. Methyl protons of the tertiary acetamido groups which split in the ranges of $\delta = 1.95$ - 2.25 ppm at room temperature, show two broad peaks with expected integral values at high temperature. Except H^k , H^l and H^8 protons, ROTa consist seven other aliphatic protons, which includes five from wheel (H^c , H^d , H^g , H^h , H^i) and two from centre piece (H^5 , H^6) that resonate between $\delta = 3.25$ to 4.50 ppm as multiplets at room temperature. But upon heating, the multiplicity of all those seven proton signals convert to seven distinguishable peaks with proper integration ratio in the range of $\delta = 3.42$ to 4.57 ppm at 393 K (Figure 60S and 61S in ESI†).

ROTB: Figure 3a clearly shows that at higher temperature, the multiplets associated with the particular peaks of ROTb are converged and resonate within a narrow range compared to the room temperature NMR spectrum. Since the aryl ring contains 4-fluoro substituent, this kind of exchange is also monitored via proton decoupled $^{19}\text{F-NMR}$ spectroscopy. ROTb shows multiple signals at the range of $\delta = -112.0$ to -114.0 ppm for the fluorine at 298 K. At 353 K, the multiple signals of $^{19}\text{F-NMR}$ is reduced to only two which can ascribed to one middle and two for terminal aryl rings (Figure 4). There are only one set of peaks (e.g. $\text{H}_{\text{Ar}}^{1,2,3,7}$, $-\text{NH}^4$) in ROTb which reveals that either there is only one conformer or the exchange is rapid. Actually, the tertiary amide groups are appended in the wheel component and the effect of rotamer induced conformational/ co-conformational variation should be more prominent in the wheel component rather than the DMBL part of the rotaxane. Thus, it is observed that the H_{Ar}^e proton

show broad and multiple peaks at room temperature [Figure 2 and 3a]. Ar-H^{l,m} are the parts of the wheel sub-component and thus the rotamer induced fluxionality should be prominent in the mentioned proton. As the aromatic protons Ar-H^{9,10,11,a,a',b,l,m} are resonating within the same ppm range, it is hard to isolate them separately. Being a part of ring component, Ar-H^l, H^m [Chart 1] should show broad or multiple peak at room temperature. Indeed, Ar-H^l, Ar-H^m show the conformational variation at room temperature.

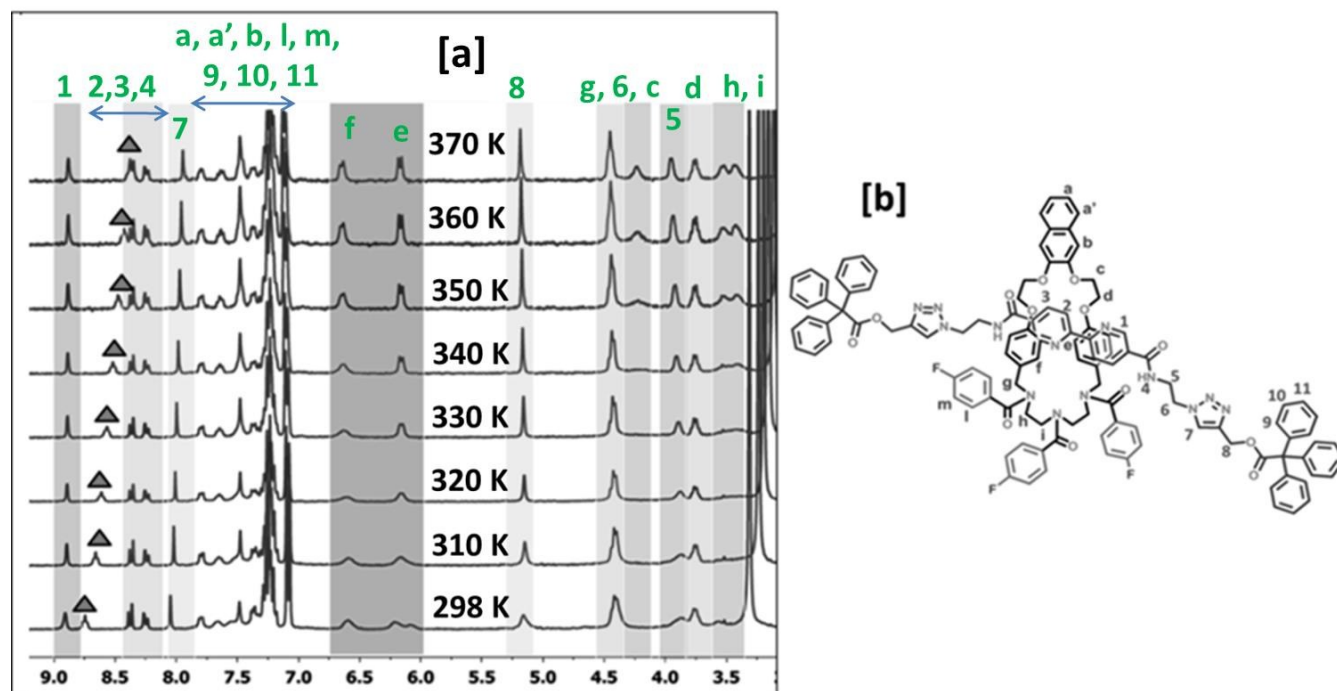


Figure 3. (a) Variable temperature ^1H -NMR spectra of ROTb in $\text{DMSO}-d_6$ at 300 MHz. The triangle indicates the upfield shifting of the amide proton peak $-\text{NH}^4$ upon increasing temperature. At 370 K, the amide proton peak $-\text{NH}^4$ merges with the aromatic proton $\text{Ar}-\text{H}^2$, (b) Chemical diagram of ROTb.

The ^{19}F -NMR spectrum shows the real scenario. As fluorine is attached with the aromatic rings of the wheel component, the ^{19}F signals show the multiplicity at room temperature (298 K) and upon heating at 353 K (high temperature) spectrum shows only two peaks (2:1 ratio) attributed to middle and terminal aryl rings (Figure 4). This supports fast inter-conversion on the NMR timescale at higher temperature.

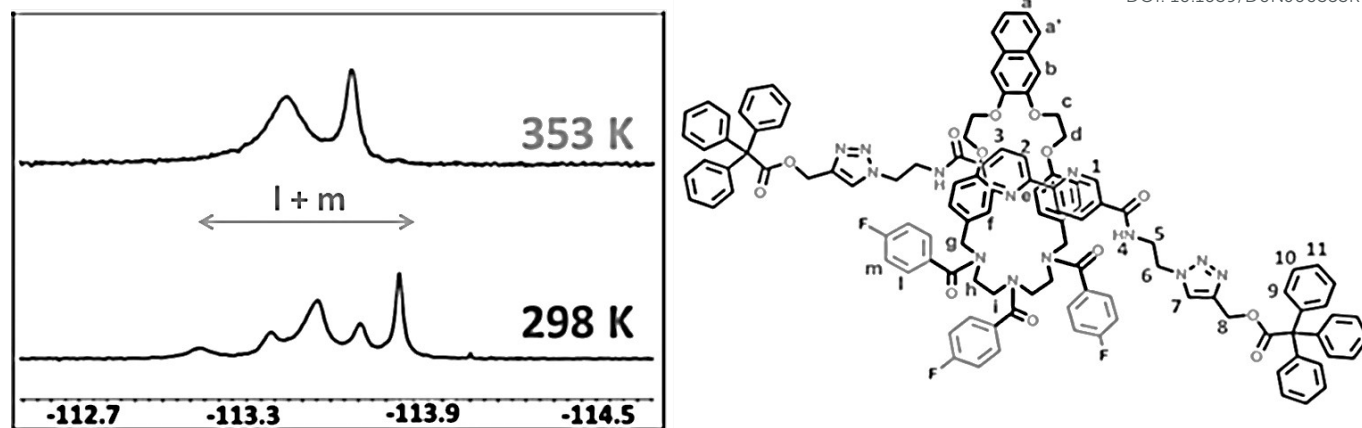


Figure 4. Proton decoupled, temperature dependant ^{19}F -NMR spectra of ROTb in $\text{DMSO-}d_6$ at 500 MHz.

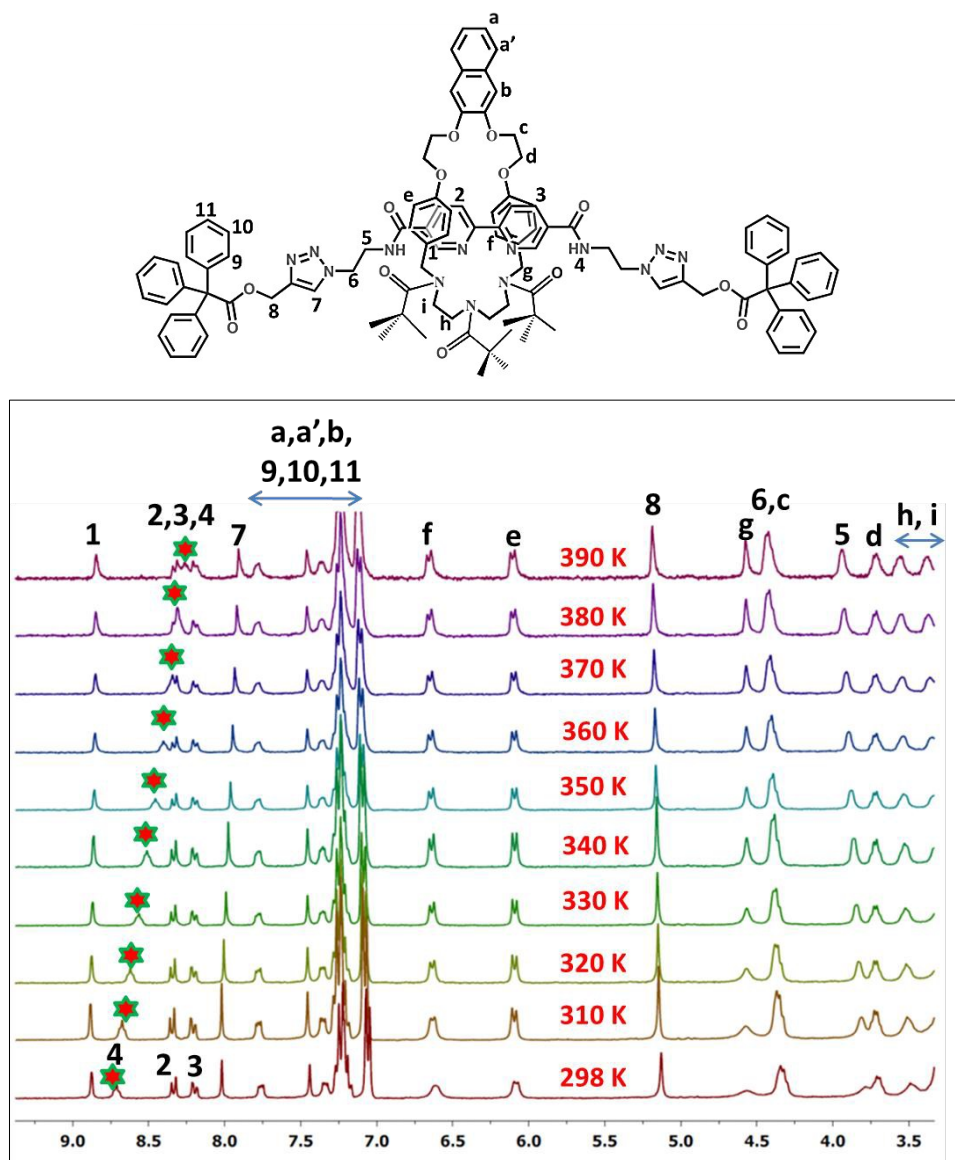


Figure 5. Variable temperature $^1\text{H-NMR}$ data of **ROTc** in DMSO-d_6 (300 MHz). The star marked proton is corresponds to the amide $-\text{NH}_4$ proton which show the upfield shift upon raising temperature

ROTc: Due to restricted rotation of the tris-tertiary butyl group appended rotaxane **ROTc**, the numbers of conformers and co-conformers are less compared to the **ROTa** and **RO Tb**. However, we have undertaken the variable temperature $^1\text{H-NMR}$ experiment of **ROTc** in DMSO-d_6 solvent system and the data analysis reveals that there is practically no significant changes are observed at higher temperature NMR data except the amide peak of the centre piece component ($-\text{NH}_4$) which is resonate around $\delta = 8.75$ ppm at 298 K and shifted to upfield with raising temperature (**Figure 5**). Low temperature NMR data also support our conclusion (**Figure 63S** and **64S** in ESI †).

Photophysical properties of rotaxanes: Absorption spectra of substituted wheels (**M Ca-c**) show peak at ~ 285 nm whereas, **RO Ta-c** show peak at the zone of 285-305 nm (**Figure 6a** for **M Cc** and **23S** in ESI † for **M Ca** and **M Cb**, **Figure 6b** for **RO Tc**). On the other side, photoluminescence spectra of macrocycles **M Ca-c** show peak at the region ~ 340 nm (excitation at 285 nm, **Figure 6c** for **M Cc** and **23S** in ESI † for **M Ca** and **M Cb**). Interestingly, bipyridyl-based axle threaded wheel i.e. rotaxanes **RO Ta-c** show altogether different photoluminescence properties than their non-interlocked counterpart **M Ca-c** (**Figure 6d**, **Figures 23S**, **59S** in ESI †) when excited at 285 nm. An additional new broad band at around ~ 470 nm is observed along with a characteristic peak of naphthyl moiety at around ~ 340 nm. However, there is no significant difference in the absorption spectra of the interlocked species when compared with their non-interlocked components (**Figure 66S-70S** in ESI †). Thus, these results reveal that the generation of such broad spectrum is an excited state phenomenon. To ascertain the nature of the broad band (intra vs. inter molecular charge transfer), we have carried out the solvent and concentration dependant photoluminescence studies of **RO Ta-c**. Experimental evidences reveal that the broad band is highly solvatochromic in nature. In fact, the broad band shifts from 491 nm in toluene to 527 nm in tetrahydrofuran, 470 nm in CH_3CN and the peak vanishes in CH_3OH . When a polar protic solvent like CH_3OH is added to the CH_3CN solution of tris-tertiary amide functionalized rotaxanes (**Figure 7a**, **7b**, and **72S-74S** in ESI †) then also the broad peak gradually diminishes, and vanishes completely after the addition of $\sim 10\%$ CH_3OH . Further, the quenching of PL-intensity shows a linear relationship with concentration (**Figure 7c**, **75S-77S** in ESI †). These set of experiments suggest that the new broad band must be arising due to an intramolecular exciplex formation and not from the intermolecular aggregation within the experimental conditions. The exciplex is expected to be formed between the electron-rich naphthyl group present in the wheel component and the electron-deficient bipyridine unit of the thread (**Figure 7e**). Even 1:1 mixtures of functionalized macrocyclic ring and the centre piece do not show the formation of such exciplex (**Figure 71S** in ESI †). Thus, it can be inferred that an electron-

rich group in the wheel and an electron deficient functionality in axle are in close proximity and is responsible for executing intra-molecular interaction in the excited state.

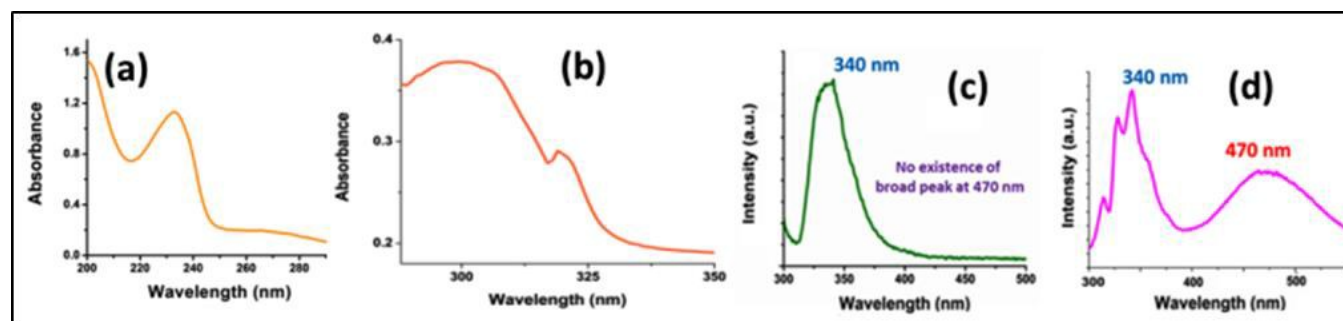


Figure 6. Absorption spectra of (a) MCc (Concentration: $1.1 \times 10^{-5} \text{ M}$) and (b) ROTc (Concentration: $1 \times 10^{-5} \text{ M}$) spectrum; Emission spectra of (c) MCc (Concentration = $3 \times 10^{-5} \text{ M}$) and (d) ROTc (Concentration: $2.9 \times 10^{-5} \text{ M}$). In all the cases analytes are excited at 285 nm in 9:1 (v/v) $\text{CH}_3\text{CN}/\text{CHCl}_3$ binary solvent mixture.

In this context, Swager et al. have reported “rotaxane exciplex” where intramolecular donor-acceptor interaction exists between “bipyridine ring containing centre piece” and “phenyl acetylene group” of the wheel counterpart.^{48 (b)} Further, the higher temperature stability of the exciplex is checked by recording the PL over a wide temperature range, i.e., from 283 K (10°C) to 348 K (75°C) in CH_3CN (Figure 7d and Figure 78S and 79S in ESI[†]).

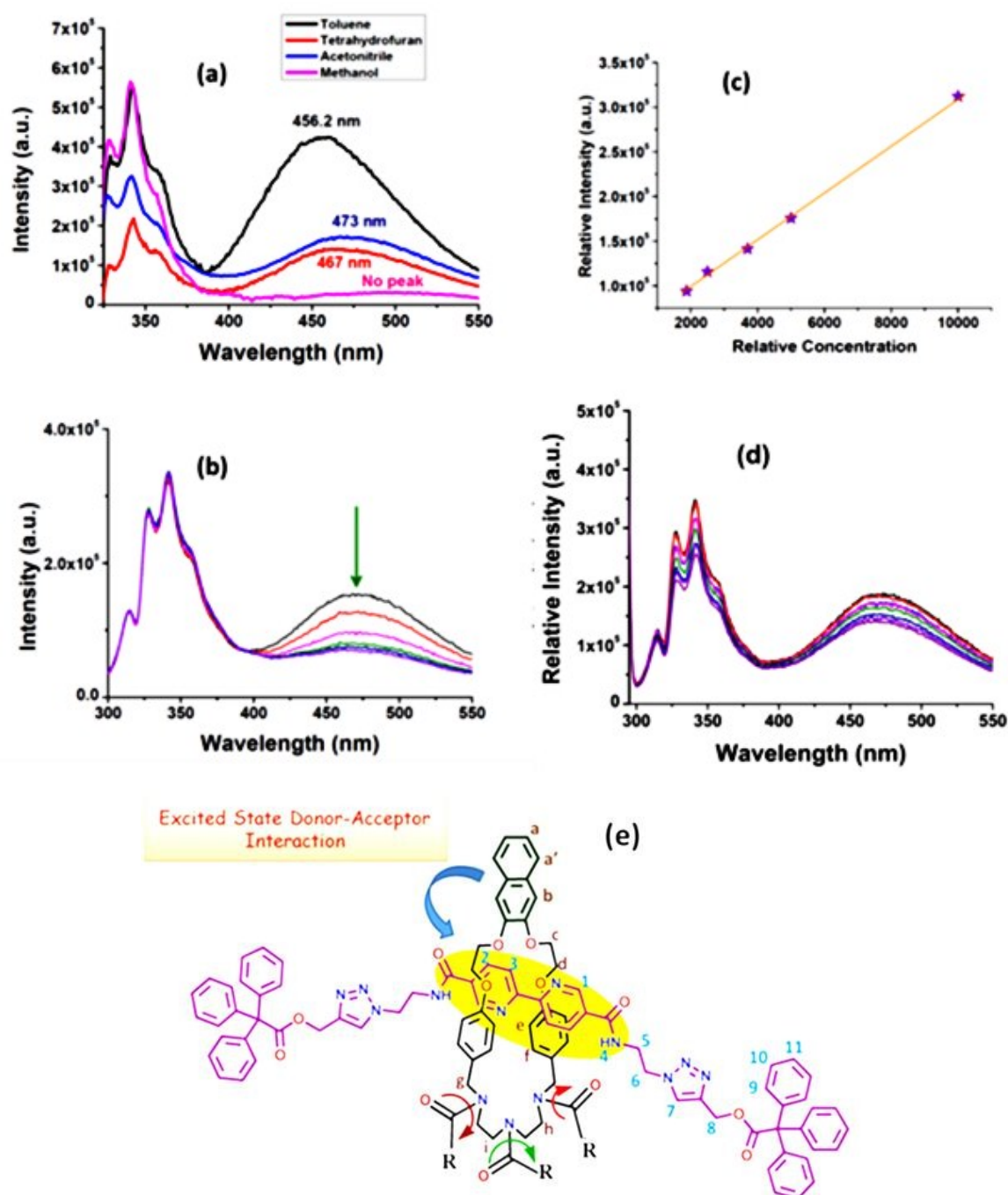


Figure 7. (a) Solvatochromic change of the exciplex peak; (b) quenching of the exciplex peak intensity upon gradual addition of polar protic solvent CH₃OH to the solution of ROTc in 9:1 (v/v) CH₃CN/CHCl₃. (c) Relative intensity vs. concentration plot upon monitoring the exciplex peak indicating the broad peak is appeared due to intramolecular donor-acceptor interaction; (d) Thermal stability of exciplex monitored through variable temperature PL studies (Spectra are recorded in 283 K, 288 K, 293 K, 298 K, 303 K, 318 K, 328 K, 348 K temperature). Concentration was taken around $2.9 \times 10^{-5} M$ for all the cases and particularly for (b), (c) and (d), 9:1 (v/v) CH₃CN/CHCl₃ binary solvent system was chosen. In every cases the solutions were excited at $\lambda_{ex} = 285 \text{ nm}$. [In these diagrams all spectra are for

1
2
3
4 *ROTC*. Same experimental data of *ROTA* and *ROTB* are presented in the ESI† section, 71S-79S in
5 ESI†], (e) Chemical diagram of *ROTA-c* with labelling showing plausible rotation around N-C(O) bond
6 and donor-acceptor interaction in the excited state which results the exciplex formation.
7
8
9

10
11 These variable temperatures PL experiment suggest that even at 353 K (80°C), the wheel and axle
12 components are present in close vicinity in *ROTA-c* which is further supported by the high temperature
13 ¹H-NMR experiments. The aromatic protons of the bipyridine moiety (H¹, H² and H³) and the rings (H^e
14 and H^f) which are resonating at upfield region upon interpenetration, remain almost unperturbed at
15 higher temperature (Figures 60S, 62S in ESI†). These set of experiments confirm that the wheel resides
16 on the bipyridine part of the axle even at higher temperature. Next, the appearance of such exciplex
17 assists to investigate the metal ion complexation property in those multi-functional rotaxanes which are
18 discussed in the later section.
19
20
21
22
23
24
25
26
27
28
29
30
31
32
33
34
35
36
37
38
39
40
41
42
43
44
45
46
47
48
49
50
51
52
53
54
55
56
57
58
59
60

Effect of Na⁺/ Cu²⁺/ Ni²⁺ on photophysical properties of rotaxanes: ¹H-NMR studies reveal regulation
of the rotamers induced kinetic activity by alkali metal ions and crown ethers in case of *ROTA* (Figure
80S in ESI†). Experimental output reveals that the accumulation of peak multiplicities in the presence
of Na⁺. Conversely, sequestering the alkali metal ion by suitable crown ether regenerates the peak
multiplicities. Details of the peak accumulation in presence of alkali metal ions are shown in the
supporting information section (Figure 80S in ESI†). This result resembles our previous reports which
indicate the coordination of alkali metal ions through the MIM has a control towards conformational/
co-conformational fixation. [In brief, we are interested to demonstrate the effect of Na⁺ on rotamer
induced dynamic behaviour (originated due to tertiary amide bonds rotation), exhibit by **ROTA** via ¹H-
NMR studies. Addition of equivalent amount Na⁺ salt solution in CD₃CN in **ROTA** in 9:1 (v/v)
CDCl₃:CD₃CN solvent mixture executes a typical accumulation of most multiplets of **ROTA**.
Comparative ¹H-NMR analysis of **ROTA** and (**ROTA** + Na)⁺ clearly indicate that the peaks corresponds
to the lateral aromatic rings of the wheel components i.e. H^e and H^f also congregate to a less number of
peaks compared to **ROTA**. Na⁺ assists to halt/retard the dynamic property upon coordinating with the
metal chelating sites present in the rotaxane. When equivalent amount of 18-crown-6 is added as an
input to the mixture of **ROTA** and Na⁺, regeneration of the multiple peaks are observed in the ¹H-NMR
spectrum. This can be easily explained upon considering the phenomenon that crown ether removes Na⁺
from the system and as a consequence of that the multiple conformations/ co-conformations again
started to exhibit.]

At this juncture, it would be appropriate to study the effect of alkali metal ion on the photoluminescence
property of fluorophoric rotaxanes which might provide relevant information on the conformational and

co-conformational fixation of this category of rotaxanes. In presence of Na^+ , there is practically no perturbation in the absorption and emission spectra (**Figure 8a** and **8b**). Thus it indicates that bipyridine unit is also not involved towards coordination with such metal ions. If Na^+ binds at the oxy-ether pocket of the ring and/ or the bipyridine unit then one would expect an obvious change in the exciplex emission intensity due to chelation. This experiment tells that the Na^+ is not binding at the oxy-ether pocket (**Figure 8c**). Then, the photophysical study of ROTa in the presence of transition metal ions such as Cu^{II} / Ni^{II} as a guest is carried out.⁷⁰

The UV/Vis study reveals the involvement of bipyridine part of the DMBL component (**Figure 8d**). As the bipyridine unit is responsible for the exciplex formation, it is expected that upon suitable metal ions coordination with the bipyridine unit, the exciplex formation might be obstructed. In fact, the PL intensity of the exciplex is decreased to a significant extent in presence of Cu^{II} and Ni^{II} which also confirms the involvement of bipyridine unit towards metal ion chelation (**Figure 8e**). Upon chelation, particularly, between Cu^{II} / Ni^{II} with bipyridine unit, the donor-acceptor interaction between naphthalene and bipyridine in the excited state is interrupted and as a result of that fluorescence quenching of the exciplex emission is observed at ~ 470 nm. One may assume the binding mode of the transition metal ions as depicted in **Figure 8f** where additional coordination may provide by the tris tertiary amide moiety.

Thus along with the sp^2 nitrogen atoms of bipyridine moiety, other coordination sites are tertiary amide N-atoms and this assumption is based on the report by Bannwarth et al.⁷² These set of experiments reveals that the probable site of the alkali metal ion coordination could be the O-atoms of tertiary amide carbonyls in exotopic mode (**Figure 8c**), not within the cavity of the wheel, whereas, transition metal ions are binding in the endotopic mode. In case of Na^+ , binding through the amide carbonyl might cause the particular preferential orientation of the acetamido group and as a result, in presence of Na^+ , conformational fixation might take place. It is important to mention that our recent report showed that even in the absence of oxy-ether group, tris-acetamido containing amide based macrocyclic wheel derived rotaxane (ROTa', chemical diagram is shown in **Figure 8IS** in ESI†) can also show conformational fixation upon addition of investigated alkali metal ions.⁶⁸

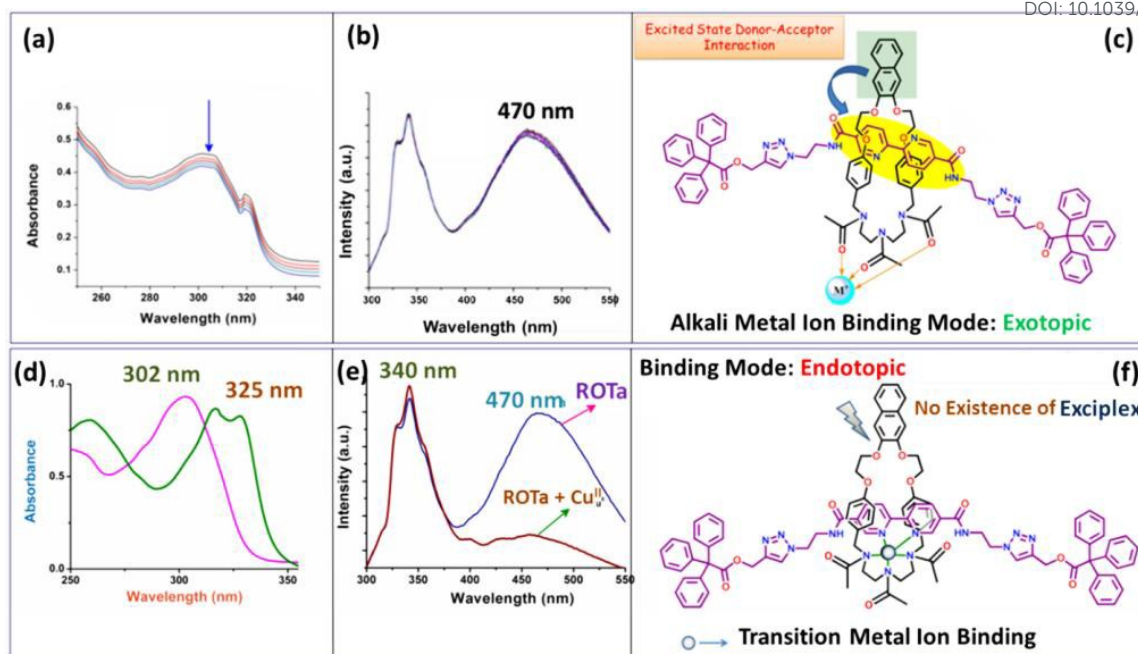


Figure 8. (a) Unperturbed absorption spectra of ROTa (1.56×10^{-5} M) in the presence of equimolar concentration of Na^+ ; (b) Unperturbed photoluminescence spectra of ROTa (1.56×10^{-5} M) in the presence of equimolar concentration of Na^+ , excited at $\lambda_{\text{ex}} = 285$ nm. (c) Exotopic binding mode of alkali metal ion through amide carbonyl; (d) perturbed absorption spectra of ROTa (1.56×10^{-5} M) in the presence of equimolar amount of Cu^{II} ; (e) photoluminescence spectra of ROTa (1.56×10^{-5} M) in the presence of equimolar amount of Cu^{II} , excited at $\lambda_{\text{ex}} = 285$ nm; (f) Endotopic binding mode of transition metal ion. In all the cases 9:1 (v/v) $\text{CH}_3\text{CN}/\text{CHCl}_3$ solvent is used.

On the other hand, report by Heinrich et al. states that the presence of proximal positive charge causes the conformational fixation of tertiary amides.⁷³

Detailed solution state transition metal ion binding with the rotaxanes: In the previous section, we have observed that ROTa binds with the transition metal ions like Cu^{II} / Ni^{II} . Thus, here we have undertaken detailed solution state studies on the metal ion coordination of MIM's using absorption and emission spectroscopy. In a typical experiment, ROTa ($\sim 10^{-5}$ M in 9:1 $\text{CH}_3\text{CN}/\text{CHCl}_3$, v/v) is used as host whereas, $\sim 10^{-4}$ M solutions of various metal ions (Ni^{II} , Co^{II} , Cu^{II} , Fe^{III} , Mn^{II} , Cr^{II}) are used as guests in CH_3CN . Upon addition of guest to the host, the red shift of the absorption bands corresponding to $n-\pi^*$ transition of the bipyridine unit are observed with a concomitant decrease of the parent absorption peak intensity at 302 nm, particularly, in cases of Cu^{II} and Ni^{II} . Interestingly, a gradual increase in the intensity of red shifted band at around 320-325 nm is observed in case of ROTa, up to the addition of 1.0 equivalent of corresponding metal salts (**Figure 9a and 9d**). Other investigated metal ions such as Fe^{II} , Mn^{II} , Cr^{III} , Na^{I} , K^{I} , Li^{I} are unable to perturb the absorption spectrum (**Figure 8**, 83S in ESI[†]). A

clear isosbestic point is maintained during the addition of 1.0 equiv of Cu^{II} and Ni^{II} . Job plot and equivalent plot analysis of these absorption spectroscopic titration data shows an inflection point at 0.5, supporting a 1:1 host-guest stoichiometric binding (**Figure 9b and 9e** and Table 1).

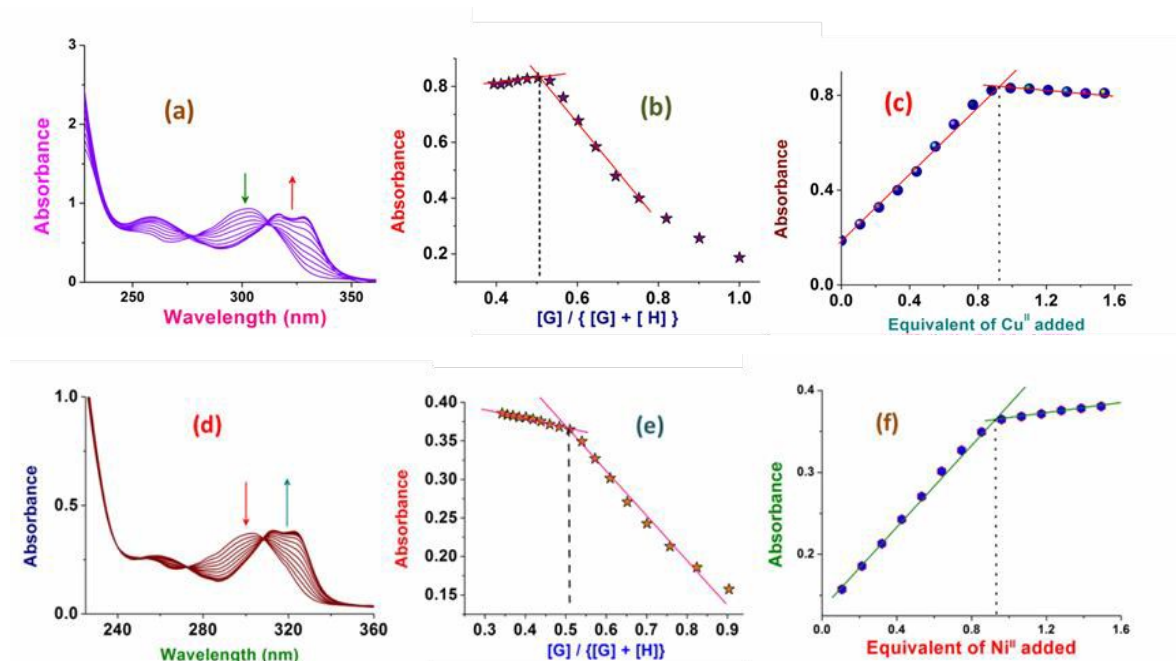


Figure 9. Absorption spectroscopic titration profile of ROTa (1.0×10^{-5} M) with (a) Cu^{II} (1.2×10^{-4} M) and (d) Ni^{II} (1.1×10^{-4} M). Job plot [Figure (b) for Cu^{II} and (e) for Ni^{II}] and Equivalent plot [Figure (c) for Cu^{II} and (f) for Ni^{II}] indicates the 1:1 stoichiometric binding. Spectra are recorded in 9:1 CH_3CN / DMF (v/v) solvent mixture.

Binding constants are calculated by using non-linear curve fit analysis which shows that association constants are $6.76 \times 10^6 \text{ M}^{-1}$, and $4.32 \times 10^6 \text{ M}^{-1}$ for Cu^{II} , and Ni^{II} as guests respectively (**Table 1** and **Figure 86S** in ESI[†]). Titration experiments have also been carried out for ROTb-c as host and above metal ions (Cu^{II} , Ni^{II} , Co^{II} , Fe^{II} , Mn^{II} , Cr^{III}) as guests in a similar way as performed for ROTa. However, here we do not observe any desirable stoichiometric binary complexation (**Figures 84S-85S** in ESI[†]). Thus UV-Vis study confers that the electron donating effect as well as steric factor play important roles towards the coordination with the transition metal ions by the tertiary amide group appended rotaxanes. Likewise, upon addition of transition metal ions to the solution of ROTa, the exciplex peak gets quenched (**Figure 10(a)** and **Figures 87S** in ESI[†]) in fluorescence spectra. No enhancement/ quenching of monomer emission intensities at 340 nm is observed in the presence of any metal ions (**Figures 87S** in ESI[†]). In fact, the PL intensity of the exciplex is decreased to a greater extent in case of Cu^{II} and Ni^{II} whereas, upon addition of higher equivalent of other transition metal ions such as Cr^{III} , Mn^{II} , Fe^{II} , Co^{II} to the solution of the respective rotaxanes (ROTa-c) quenching of exciplexes have been observed

(Figures 87S-89S in ESI†). These observations exemplify that facile complexation with stoichiometric ratios is obtained only in case of Cu^{II} and Ni^{II} which reflects the trends of Irving-William series.

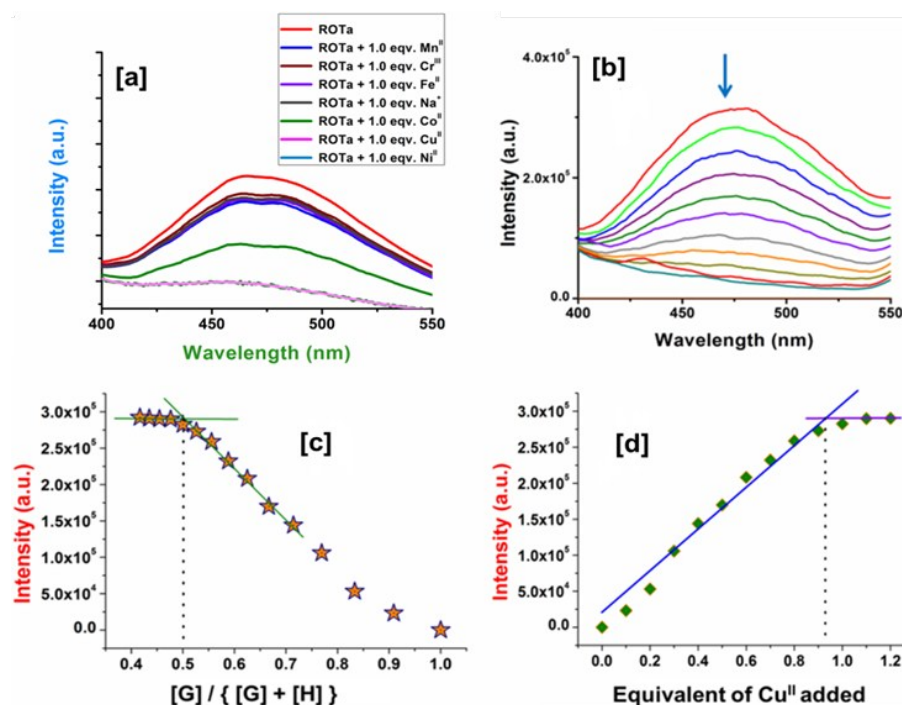


Figure 10. (a) Comparative photoluminescence spectra of ROTa ($3.0 \times 10^{-5} \text{ M}$) with equivalent amount of (i) Mn^{II} , (ii) Cr^{III} , (iii) Fe^{II} , (iv) Na^+ , (v) Co^{II} , (vi) Cu^{II} and (vii) Ni^{II} in 9:1 $\text{CH}_3\text{CN}/\text{CHCl}_3$ binary solvent mixture. (Excited at $\lambda_{\text{ex}} = 285 \text{ nm}$); (b) PL titration profile ROTa ($3.0 \times 10^{-5} \text{ M}$) with Cu^{II} in CH_3CN . (b) Job plot, and (c) equivalent plot for ROTa ($3.0 \times 10^{-5} \text{ M}$) with Cu^{II} ($2.89 \times 10^{-4} \text{ M}$) in CH_3CN at 25°C (Excited at $\lambda_{\text{ex}} = 285 \text{ nm}$.)

Table 1. Stoichiometry and association constant of metal ion complexation using ROTa host

Guest	Inflection point from Job plot	Host: Guest Stoichiometry	Association Constant (M^{-1})
Cu^{II}	~ 0.5	1:1	6.76×10^6
Ni^{II}	~ 0.5	1:1	4.32×10^6

However in cases of both ROTb and ROTc, quenching of the exciplex peak intensity (Figures 88S, 89S in ESI†) are observed as obtained in case of ROTa. This could be due to the interaction of bipyridine unit with the metal ions which eventually disrupts the exciplex interaction as shown in Figure 8. Thus, the involvement of bipyridine unit towards metal ion chelation and inhibition of the excited state donor-acceptor interactions occur fully in a synergistic way. Our previously published results show that the

1
2
3
4 macrocycle, metal ion and axle form 1:1:1 ternary complexes via pseudorotaxane formations.^{60,62} In
5
6 this present study, potential redox quenching of luminescence may also occur but it is evident from our
7
8 previous studies that the Cu^{II} and Ni^{II} act as a potential candidate to act as guest and such binding is
9
10 examined upon monitoring the band of bipyridine via absorption spectroscopy. In this case also, upon
11
12 monitoring the bipyridine reveals the 1:1 binary complexation between functionalised rotaxane (ROTa)
13
14 and metal ion, particularly with Ni^{II} and Cu^{II}. One might assume that only bipyridine is involved in
15
16 binding along with the solvent molecules or the tris amide pockets are also involved towards
17
18 coordination. Whatever might be the case, absorption spectroscopic studies indicate that the bipyridine
19
20 unit is involved towards metal ion coordination and thus hamper the exciplex formation.

21 22 Conclusions

23
24 A family of tertiary amide group appended multifunctional rotaxanes having complementary wheel and
25
26 axle components displays the excited state donor-acceptor interaction. Structure property studies are
27
28 exemplified upon varying bulkiness of the group that is attached to tertiary amide centers. Readable
29
30 dynamic properties are imposed due to the N-C(O) bond rotation which can be regulated by increasing
31
32 the bulkiness of the appended groups. On the other hand, conformational fixation of tri-acetylated
33
34 rotaxane can be achieved by Na⁺ as an input. The exciplex formation in rotaxane is also utilized for the
35
36 mechanistic investigation of Na⁺ assisted conformational/ co-conformational fixation. Photophysical
37
38 studies show the coordination of alkali metal ion through exotopic binding fashion of the tri-acetylated
39
40 rotaxane whereas; transition metal ions prefer endotopic coordination. Metal ion coordination behaviors
41
42 are also dependent on the substitution effects. Cu^{II} and Ni^{II} are found to be the choice of metal ions for
43
44 the coordination of tri-acetylated rotaxane, ROTa. Attachment of tertiary amide group on MIM's and
45
46 their dynamic controls are helpful towards the future development of more functionalized molecular
47
48 machines and the exciplex forming nature can be utilized towards sensing, recognition and overall
49
50 monitoring of the molecular machinery track by photophysical output.

51 52 Experimental Section and General Details:

53
54 All the reagents were obtained from commercial suppliers such as Sigma Aldrich, Merck, Alfa Aesar,
55
56 and Spectrochem, India and are used as received without further purification. 2,2'-bipyridine 5,5'-diacid,
57
58 its di-acid chloride derivative and the bis-azide terminated axle **AXL**, were synthesized using
59
60 previously reported procedure.^{60,75} Peak assignments in the ¹H NMR spectra were confirmed by using
COSY, NOESY, ROESY NMR spectra of the compounds. In every cases of PL experiment, we have
excited at 285 nm which states that irradiation at 285 nm, the maximum of the wavelength in the PL
spectrum should be originally visualised at around 342 nm on the basis of the naphthalene ring.

Materials: All reactions were carried out in a dry argon gas atmosphere, and workup procedures were carried out under ambient conditions. Acetonitrile, dichloromethane was refluxed over CaH_2 and was collected prior to use. THF was dried by using Na-metal. Metal salts having perchlorate counter anions, diethylene triamine, 4-fluoro benzoyl chloride, 5,5' dimethyl 2,2'-bipyridyl, were purchased from Aldrich and were used as received. Ethanol, 2,3-dihydroxy benzene, 4-hydroxy benzaldehyde, 1,2-dibromoethane, potassium carbonate, sodium borohydride, pivoyl chloride, thionyl chloride, 2-bromo ethylamine hydrobromide, boc-anhydride, trifluoro acetic acid were purchased from Spectrochem Pvt. Ltd., India. Potassium dichromate, potassium bicarbonate, sodium azide were procured from Merck.

Methods. HRMS analysis was performed on a QToF-Micro YA 263 mass spectrometer in positive ESI mode. ^1H , ^{13}C , DOSY, COSY, NOESY, ROESY, HSQC -NMR experiments were carried out on FT-NMR Bruker DPX 300/ 400/ 500 MHz NMR spectrometer. Variable temperature ^1H -NMR experiments were carried out on a 300 MHz Bruker DPX NMR spectrometer. Chemical shifts for ^1H , ^{13}C , and ^{19}F -NMR were reported in parts per million (ppm), calibrated to the residual solvent peak set. Absorption spectra were recorded in a Perkin Elmer Lambda 900 UV/ vis/ NIR spectrophotometer (with a quartz cuvette of path length 1 cm), and emission spectra were recorded in a Fluoro Max-3 spectrophotometer, from Horiba Jobin Yvon. Elemental analysis was performed on PerkinElmer 2500 series II elemental analyzer, PerkinElmer, USA. Caution! Perchlorate salts of the both alkali and transition metal ions and organic azide are explosive under certain conditions, particularly when these salts/ compounds are used in large amount and certain amount of heat energy was provided. All precautions should be taken during the course of handling such chemicals.

Synthetic Procedures:

(a) Synthesis of compound I:

In a 250 mL R.B. excess 1, 2-dibromoethane (2.15 mL, 25.0 mmol, 5.0 eqv.) was added to the solution of 4-hydroxybenzaldehyde (0.610 g, 5mmol, 1.0 eqv.) in the presence of K_2CO_3 (2.1 g, 15.0 mmol, 3.0 eqv.). The reaction mixture was then refluxed for 24h under inert condition having CH_3CN as solvent. Then the crude reaction mixture was dried under vacuum and extracted with CHCl_3 and water. The resultant organic layer was repeatedly washed with saturated brine solution. The organic layer was dried over vacuum. The CHCl_3 part was evaporated, and the yellow oily product was purified by column chromatography by using 94:6 hexane/ ethyl acetate and using silica gel (60-120 mesh) as a stationary phase to obtain the white crystalline product (930.5 mg, Yield 82%). The purity of the compound was checked by NMR and ESI-MS which matches well with previously reported data. ^{61}H NMR (400 MHz, CDCl_3): δ (ppm) 4.45 (s, 4H, $-\text{CH}_2$), 7.05 (d, 2H, $J = 8$ Hz, Ar-H), 7.85 (d, 2H, $J = 8$ Hz, Ar-H), 9.91 (s,

1H, Ar-CHO). ¹³C NMR (75 MHz, CDCl₃): δ (ppm) 28.7, 67.9, 114.8, 130.4, 131.9, 130.3, 162.9, 190.6.

(b) Synthesis of compound II:

2,3-dihydroxy naphthalene (0.16 g, 1.0 mmol, 1.0 eqv.) was treated with compound I (0.48 g, 2.1 mmol, 2.1 eqv.) in the presence of anhydrous K₂CO₃ (0.40 g, 3.0 mmol, 3.0 eqv.) having CH₃CN as a solvent. The reaction mixture was refluxed for 24h under an inert atmosphere at 80°C. After the completion of the reaction, the resulting solution was poured into ice cold solution and a white precipitated was formed which was collected by filtration. Yield 0.38 g, 85%. M.P. 115° C, ESI-MS (+ve): m/Z calculated for C₂₈H₂₄O₆ = 456.1573, Found 456.1632. ¹H NMR (400 MHz, CDCl₃): δ (ppm) 4.46-4.51 (m, 8H, -CH₂), 7.04 (d, 4H, J = 8.4 Hz, Ar-H), 7.24 (s, 2H, Ar-H), 7.35-7.38 (m, 2H, Ar-H), 7.68-7.70 (m, 2H, Ar-H), 7.80 (d, 4H, J = 8.8 Hz, Ar-H), 9.86 (s, 2H, Ar-CHO). ¹³C NMR (75 MHz, CDCl₃): δ (ppm) 67.0, 67.7 (4C, -CH^{c+d}), 109.7 (2C, Ar-C-H) 115.2 (4C, Ar-C), 124.8 (2C, Ar-C), 126.6 (2C, Ar-C), 129.7 (2C, Ar-C quaternary), 130.5 (2C, Ar-C quaternary), 132.1 (4C, Ar-C-H), 148.9 (2C, Ar-C-quaternary), 163.8 (2C, Ar-C-quaternary), 190.8 (C=O). Analytical Calculated for C₂₈H₂₄O₆: C: 73.67; H: 5.30; O: 21.03. Found: C: 73.52; H: 5.42, O: 21.40.

(c) Synthesis of MC:

In a 1 L two neck round bottomed flask, fitted with two pressure equalizer, one contains compound II (0.456 g, 1.0 mmol, 1.0 eqv.) in 1:1 50 mL CH₂Cl₂/CH₃OH solvent and another with diethylenetriamine (0.1 mL, 1.0 mmol, 1.0 eqv.) dissolved in 50 mL of CH₃OH. Then both of them were added drop wise to the R.B. containing a large amount of 1:1 CH₂Cl₂/CH₃OH binary solvent mixture. The addition was continued with the specific time interval for 2 days. After complete addition of both the two reagents, a macrocyclic compound was formed via imine bond formation. Then the resultant reaction mixture was allowed to stir at room temperature for 24h, and the two imine bonds were reduced by using NaBH₄ (150 mg, 4.0 mmol, 4.0 eqv.). After stirring it for additional 6h, the reaction mixture was evaporated, and the resultant solid was dissolved in CHCl₃ and washed thoroughly with water followed by brine solution. Then the separated organic phase was dried over anhydrous Na₂SO₄. A white solid compound was obtained as the product. Yield 370 mg, 70%. M.P. 170° C, ESI-MS (+ve): m/Z [(M+1)⁺] calculated for C₃₂H₃₈N₃O₄: 528.2862, Found: 528.2858; FTIR in KBr disc (v/cm⁻¹): 3429, 2921, 2852, 1606, 1510, 1249, 1174, 1116, 1060, 750; ¹H-NMR (300 MHz, CDCl₃) δ (ppm) = 2.83 (b, 8H, -CH₂), 3.70 (s, 4H, Ar-CH₂), 4.43 (m, 8H, -CH₂), 6.84 (d, 4H, J = 9.0 Hz, Ar-H), 7.16 (d, 4H, J = 9.0 Hz, Ar-H), 7.25 (m, 2H, Ar-H), 7.37 (m, 2H, Ar-H), 7.68 (m, 2H, Ar-H). ¹³C-NMR (75.47 MHz, CDCl₃) δ (ppm) = 48.2 (2C, aliphatic-CH₂), 48.6 (2C, aliphatic -CH₂), 53.3 (2C, Ar-CH₂, aliphatic), 67.4 (2C, aliphatic, -OCH₂CH₂O-), 68.5 (2C, aliphatic -OCH₂CH₂O-), 110.1 (2C, Ar-C) 115.1 (4C, Ar-C), 124.6 (2C, Ar-C),

126.6 (2C, Ar-C), 129.5 (4C, Ar-C), 129.8 (2C, Ar-C, quaternary), 133.0 (2C, Ar-C, quaternary), 149.5 (2C, Ar-C, quaternary), 158.2 (2C, Ar-C, quaternary). Anal. calculated for $C_{32}H_{37}N_3O_4$: C, 72.84; H, 7.07; N, 7.96. Found: C, 72.48; H, 6.95; N, 8.09.

(d) Synthesis of acetylated macrocycle, MCA:

MC (104 mg, 2.0 mmol, 2 eqv.) was taken in the 50 mL R.B., and dry CH_2Cl_2 was added. Then triethyl amine (1.4 mL, 10.0 mmol) was added as base to the reaction mixture. After stirring for 10 -15 minutes at room temperature, 7.0 equivalent distilled acetic anhydride (0.662 mL, 0.70 mmol) was added in the reaction mixture and was allowed to stir at room temperature for another 8 hour. Then the reaction mixture was poured into a 100 mL separating funnel and washed with distilled water and brine solution for 3-4 times respectively. The organic solvent was evaporated under reduced pressure to obtain tri-acetylated MC, MCA as a white powder. Yield 118 mg (91%). M.P. 198° C, MALDI-MS: m/Z calculated for $C_{38}H_{44}N_3O_7Na$ $[M+Na]^+$, 676.7537, found 676.786. FTIR in KBr disc (v/cm^{-1}): 3433, 2923, 2854, 1745, 1633, 1510, 1448, 1413, 1367, 1290, 1253, 1178, 1112, 1066, 946, 811, 746, 671; 1H -NMR in $CDCl_3$ (300 MHz, 298K) (mixture of rotamers), δ (ppm) 2.05-2.23 (m, 9H, $-C(O)CH_3^k$), 3.10-3.31 (m, 8H, $-CH_2^{h+i}$), 4.36-4.43 (m, 12H, $-CH_2^{c+d+g}$), 6.8-7.24 (m, 10H, Ar-H $^{e+f+b}$), 7.32 (b, 2H, Ar-H $^{a/a'}$), 7.69 (b, 2H, Ar-H $^{a'/a}$). 1H -NMR in DMSO- d_6 (300 MHz, 298K) (mixture of rotamers), δ (ppm) 1.96-2.12 (m, 9H, $-C(O)CH_3^k$), 3.10-3.31 (m, 8H, $-CH_2^{h+i}$), 4.37-4.47 (b, 12H, $-CH_2^{c+d+g}$), 6.97-7.13 (m, 8H, Ar-H $^{e+f}$), 7.32-7.36 (m, 2H, Ar-H $^{a/a}$), 7.40 (s, 2H, Ar-H b), 7.40 (m, 2H, Ar-H $^{a/a'}$). ^{13}C -NMR (75.47 MHz, $CDCl_3$) δ (ppm) = 21.5 (9C, aliphatic $-CH_3$), 29.5-31.8 (4C, aliphatic, $-NHCH_2CH_2NH-$), 44.1-46.2 (2C, aliphatic, Ar- CH_2), 67.5-68.4 (4C, aliphatic, $-OCH_2CH_2O-$) 108.6-109.2 (Ar-C), 115.5 (Ar-C), 124.9 (Ar-C), 126.8 (Ar-C), 128.2-131.4 (Ar-C), 149.1 (Ar-C), 158.5-158.8 (Ar-C), 161.2 (Ar-C), 170.4 (Ar-C). Anal. Calculated for $C_{38}H_{43}N_3O_7$: C, 69.81; H, 6.63; N, 6.43; found: C, 69.72; H, 6.45; N, 6.55.

(e) Synthesis of triaryl ring substituted, MCb:

MC (104 mg, 2 mmol, 1.0 eqv.) was dissolved in dry CH_2Cl_2 in a 50 mL R.B. flask and 10.0 equivalent triethyl amine (1.4 mL, 10.0 mmol., 5.0 eqv.) was added in the reaction mixture. Then the reaction mixture was allowed to stir at room temperature for 10 min. After that, 4-fluorobenzoyl chloride (0.95 mL, 8.0 mmol, 4.0 eqv.) was dissolved in dry CH_2Cl_2 and taken in a 25 mL pressure equalizing dropping funnel and attached with the R.B. flask. The solution of acid chloride was then added dropwise to the solution of MC in R.B. flask at 0°C under inert atmosphere. After the complete addition the reaction mixture was allowed to stir at room temperature for 12 h. Then the reaction mixture was

1
2
3
4 poured into a 100 mL separating funnel and washed with plenty of water, saturated sodium bicarbonate
5 solution and brine solution for 2-3 times respectively. Then the organic layer was dried over anhydrous
6 Na_2SO_4 . The organic phase was evaporated under reduced pressure to obtain aryl ring appended
7 functionalized wheel, MCb as a white powder. Yield 152 mg (79%). M.P. above 200° C, ESI-MS (+ve
8 mode): m/Z calcd. for $\text{C}_{53}\text{H}_{46}\text{F}_3\text{N}_3\text{NaO}_7$ $[\text{M}+\text{Na}]^+$, 916.3186, found 916.3190. FTIR in KBr disc
9 (v/cm^{-1}): 3434, 3068, 2923, 2854, 1633, 1606, 1546, 1510, 1454, 1419, 1299, 1247, 1176, 1163, 1120,
10 1099, 1062, 945, 848, 821, 757, 671, 599, 584; $^1\text{H-NMR}$ in CDCl_3 (300 MHz, 298K) (mixture of
11 rotamers), δ (ppm) 3.44 (b, 8H, $-\text{CH}_2^{\text{h+i}}$), 4.50 (b, 12H, $-\text{CH}_2^{\text{c+d+g}}$), 7.09-7.43 (b, 22H $^{\text{m+l+e+f+b+a}}$
12 $^{\text{a'}}$), 7.74-7.77 (m, Ar-H, 2H $^{\text{a' / a}}$). $^1\text{H-NMR}$ in DMSO-d_6 (300 MHz, 298K) (mixture of rotamers), δ
13 (ppm) 3.26 (b, 8H, $-\text{CH}_2^{\text{h+i}}$), 4.26-4.58 (b, 12H, $-\text{CH}_2^{\text{c+d+g}}$), 7.02-7.41 (m, 12H, Ar-H $^{\text{e+f+1+m+a/a}}$)
14 7.76 (s, 2H, Ar-H $^{\text{a' / a}}$). $^{13}\text{C-NMR}$ in CDCl_3 (300 MHz, 298K) (mixture of rotamers), δ (ppm) = 28.8,
15 29.8, 43.1, 46.9, 53.2, 67.1, 68.1, 109.0, 115.4-116.0, 124.7, 126.7, 128.7, 129.2, 131.8, 149.1, 159.0,
16 161.8, 165.1, 171.4. Anal. Calculated for $\text{C}_{53}\text{H}_{46}\text{F}_3\text{N}_3\text{O}_7$: C: 71.21; H: 5.19; N: 4.70; Found: C: 71.56,
17 H: 5.45, N: 4.59.

18 (f) Synthesis of rotaxane, MCc:

19 MC (104 mg, 2 mmol, 1.0 eqv.) was dissolved in dry CH_2Cl_2 in a 50 mL R.B. flask and 10.0 equivalent
20 triethyl amine (1.4 mL, 10.0 mmol., 5.0 eqv.) was added in the solution. Then the reaction mixture was
21 allowed to stir at room temperature for 5 min. After that, trimethylacetyl chloride/ pivaloyl
22 chloride (0.99 mL, 8.0 mmol, 4.0 eqv.) was dissolved in dry CH_2Cl_2 and taken in a pressure equalizing
23 dropping funnel. The solution of acid chloride was then added dropwise to the MC present in R.B. flask
24 at 0°C under inert atmosphere. After the complete addition, the reaction mixture was allowed to
25 vigorous stirring at room temperature for 10 h. Then the reaction mixture was poured into a 100 mL
26 separating funnel and washed with water, saturated solution of sodium bicarbonate and brine for 2-3
27 times, respectively. Then the organic layer was collected and dried over anhydrous Na_2SO_4 . The organic
28 phase was evaporated to obtain functionalized wheel, MCc as a white powder. Yield 140 mg (89%).
29 M.P. above 200° C, ESI-MS (+ve mode): m/Z calcd. for $\text{C}_{47}\text{H}_{61}\text{N}_3\text{O}_7\text{Na}$ $[\text{M}+\text{Na}]^+$, 802.4407, found
30 802.2400. FTIR in KBr disc (v/cm^{-1}): 3431, 2923, 2854, 1745, 1635, 1510, 1473, 1442, 1251, 1157,
31 372; $^1\text{H-NMR}$ in CDCl_3 (300 MHz, 298K) (mixture of rotamers), δ (ppm) 1.24 -1.35, (m, 9H,
32 $\text{C}(\text{O})(\text{CH}_3)_3$), 3.24 (b, 8H, $-\text{CH}_2^{\text{h+i}}$), 4.37- 4.38 (m, 8H, $-\text{CH}_2^{\text{c+d}}$), 4.67 (s, 4H, Ar- CH_2^{g}), 6.95-7.21
33 (m, 10H, Ar-H $^{\text{e+f+b}}$), 7.34-7.36 (m, 2H, Ar-H $^{\text{a' / a}}$), 7.67-7.70 (m, 2H, Ar-H $^{\text{a' / a}}$). $^1\text{H-NMR}$ in DMSO-
34 d_6 (300 MHz, 298K) (mixture of rotamers), δ (ppm) 1.30 (m, 9H, $\text{C}(\text{O})(\text{CH}_3)_3$), 4.08, 4.36-4.43 (b, 8H, $-\text{CH}_2^{\text{h+i}}$),
35 4.62 ((b, 4H, Ar- CH_2^{g})), 7.01 (b, 8H, Ar-H $^{\text{e+f}}$), 7.36 (b, 2H, Ar-H $^{\text{a' / a}}$), 7.41 (s, 2H, Ar-H $^{\text{b}}$),
36 7.77 (b, 2H, Ar-H $^{\text{a' / a}}$). $^{13}\text{C-NMR}$ (CDCl_3) δ (ppm) = 28.5 (9C, aliphatic, $-\text{CH}_3$), 29.7 (3C, aliphatic,
37 quaternary), 39.2 (4C, aliphatic, $-\text{NHCH}_2\text{CH}_2\text{NH}-$), 45.9-46.4 (2C, aliphatic, Ar- CH_2), 67.7-68.2 (4C,

aliphatic, -OCH₂CH₂O-), 109.3 (Ar-C), 115.7 (Ar-C), 124.5 (Ar-C), 126.5 (Ar-C), 128.3 (Ar-C, two signals merged here), 129.6 (Ar-C), 149.2 (Ar-C), 158.7 (Ar-C), 178.3 (3C, C=O). Anal. calculated for C₄₇H₆₁N₃O₇: C, 72.37; H, 7.88; N, 5.39; found C, 72.65; H, 7.95; N, 5.56.

(g) Synthesis of bis-azido bis-amido 5,5'- bipyridyl based axle, AXL: The axle was made by following our literature procedure, and the characterization data were matched with the literature report.⁶⁹

(h) Synthesis of the stopper, STP: STP was prepared by our published synthetic protocol.⁶¹

(i) Synthesis of [2]pseudorotaxane, PROT:

A solution of Ni(ClO₄)₂ · 6H₂O (73 mg, 0.2 mmol) in CH₃OH (5 mL) was added to a solution of MC (114.2 mg, 0.2 mmol) in CH₃OH/CH₂Cl₂ (1:1, 5 mL) at room temperature. After stirring for it for 0.5 h, the solid di-azide axle AXL (76 mg, 0.2 mmol) was added to the reaction mixture and few drops of CH₃CN was added in the reaction mixture. During the course of the reaction, the suspension became clear. Then the resultant mixture was stirred for another 4h, and the solvent was evaporated to dryness. The greenish yellow solid was repeatedly washed with CH₂Cl₂ and dried in vacuum to obtain pure product PROT, yields: 185 mg (76%).M.P. above 200° C. The complex is characterized by absorption spectroscopy and ESI-MS spectrometry. ESI-MS (+ve): m/Z calculated for C₄₈H₅₃ClN₁₃NiO₁₀, 1064.30, found 1064.27. Anal. Calculated for C₄₈H₅₃Cl₂N₁₃NiO₁₄:C, 49.46; H, 4.58; N, 15.62, found: C, 49.92; H, 4.22, N, 15.88. FTIR in KBr disc (v/cm⁻¹): 3371, 3353, 2102, 1660, 1608, 1510, 1446, 1251, 1114, 1076, 946, 852, 756, 626.

(j) Synthesis of [2]rotaxane, ROT':

Azide terminated PROT (0.24 g, 0.2 mmol, 1.0 eqv.) was dissolved in 1:1 de-gassed CH₂Cl₂/CH₃CN binary solvent mixture inside the glove box. The alkyne-terminated stopper unit, STP (0.143 g, 0.44 mmol, and 2.2eqv.) was dissolved in CH₂Cl₂ and added to the stirring solution of PROT. Then Na₂CO₃ (0.010 g) was added as a solid, followed by the addition of tetrakis (acetonitrile) copper(I) hexafluorophosphate, Cu(CH₃CN)₄PF₆ solution in CH₃CN (75 mg, 0.2 mmol, 2.0 eqv.) to the reaction mixture. The reaction was stirred for 12h inside the glove box at room temperature. Then the resulting mixture was taken off from the glove box and evaporated to remove CH₂Cl₂/CH₃CN. A saturated solution of Na₂EDTA (10 mL) in water was added to the resultant crude and stirred for 48h to remove the metal ions. The solution was suspended in CHCl₃ in a separating funnel and washed with plenty of water followed by saturated brine solution. Then the organic layer was evaporated under vacuum to obtain a yellowish solid. The resulting solid was used as a precursor to synthesize boc protected rotaxane.

The crude reaction mixture was taken in a 50 mL R.B. and dissolved in dry CH_2Cl_2 . Then triethyl amine (0.139 mL, 1.0 mmol, 5.0 eqv.) was added in it. After stirring for 10-15 min, excess di-tertiary butyl dicarbonate (0.229 mL, 1.0mmol, 5.0 eqv.) was added in the reaction mixture. Then the mixture is allowed to stir at room temperature for 4h under an inert atmosphere. After that, the solvent was evaporated and purified by preparative TLC by using 1-3% $\text{CH}_3\text{OH}/\text{CH}_2\text{Cl}_2$ as eluent and silica gel GF-254 as a stationary phase to afford 162 mg (43%) of the targeted metal free boc-protected [2]rotaxane ROT', along with dumbbell-shaped component DMBL. Yield: 72 mg (35%). These processes were repeated to synthesize large amount of ROT' for next steps. ESI-MS (+ve): m/z calcd. for $\text{C}_{109}\text{H}_{113}\text{N}_{13}\text{O}_{16}\text{Na} [\text{M}+\text{Na}]^+$, 1884.13, found 1884.46. $^1\text{H-NMR}$ (CDCl_3 , 500 MHz): δ (ppm) 1.43, 3.44, 3.82, 3.93, 3.98, 4.33, 5.24, 6.05-6.14, 6.74, 7.13-7.44, 7.65, 8.13-8.32, 8.41, 8.72.

The main aim was to remove the DMBL and wheel component from the interlocked components. This compound was used for the next steps without high degree of purification. $^1\text{H-NMR}$ spectra and ESI-MS spectra were recorded and the data were given in the SI section that helps to predict the formation of interlocked components.

(k) Synthesis of acetylated rotaxane, ROTa:

[2]rotaxane, ROT' (186 mg, 0.1 mmol, 1.0 eqv.) was dissolved in dry CH_2Cl_2 in a 50 mL R.B. flask and 10.0 equivalent of trifluoroacetic acid (0.076 mL, 1.0 mmol, 10.0 eqv.) is added in the reaction mixture. Then the resultant solution was allowed to stir at room temperature for 12h. The solvent along with the excess acid was evaporated to obtain a sticky mass which mainly contains protonated rotaxanes with trifluoro acetate counter anions. The crude product (TROT) was used in the next step without further isolation and purification.

To the sticky mass of TROT which was obtained in the 50 mL R.B., dry CH_2Cl_2 was added. Then excess triethyl amine (0.70 mL, 5.0 eqv. with respect to the trifluoro acetic acid) was added to the reaction mixture. After stirring for 10 minutes at room temperature, 3.5 equivalent distilled acetic anhydride (0.035 mL, 0.35 mmol, 3.5 eqv.) was added in the reaction mixture and was allowed to stir at room temperature for another 6h. Then the reaction mixture was poured into a 100 mL separating funnel and washed with plenty of water and brine solution for 2-3 times respectively. The organic phase was evaporated under reduced pressure to obtain tri-acetylated [2]rotaxane, ROTa as a white powder. Yield 142 mg (84%). M.P. above 200°C . ESI-MS (+ve mode): m/Z calculated for $\text{C}_{100}\text{H}_{96}\text{N}_{13}\text{O}_{13} [\text{M}+\text{H}]^+$, 1687.7284, found 1687.7278. . FTIR in KBr disc (v/cm^{-1}): 3407, 2923, 2852, 1728, 1658, 1635, 1596, 1548, 1446, 1384, 1296, 1238, 1172, 1114, 1053, 950, 746. $^1\text{H-NMR}$ in CDCl_3 (300 MHz, 298K) (mixture of rotamers), δ (ppm) = 1.88-2.2 (m, 9H, $-\text{CH}_3^{\text{k}}$), 3.4-3.9 (m, 16H, $\text{CH}_2^{\text{h+i+5+d}}$), 4.3 – 4.5 (m, 12H, $-\text{CH}_2^{\text{6+g+c}}$), 5.22 – 5.37 (m, 4H, $-\text{CH}_2^{\text{8}}$), 6.00 - 6.17 (m, 4H, Ar-H^e), 6.73 -6.80 (m, 4H, Ar-H^f), 7.16-7.24 (m, 34H, Ar-H^{9+10+11+a/a'+b}), 7.38-7.41 (m, 2H, Ar-H⁷), 7.41 – 7.51 (m, 2H, $-\text{NH}^{\text{4}}$),

7.71 (b, Ar-H, Ar-H^{a'/a}), 8.23-8.30 (m, 4H, Ar-H²⁺³), 8.65-8.76 (m, 2H, Ar-H¹). ¹H-NMR in DMSO-d₆ (500 MHz, 298K) (mixture of rotamers), δ (ppm) 1.88-2.25 (m, 9H, -CH₃^k), 3.44-3.71 (m, 12H, CH₂^{h+i+5}), 3.89-3.94 (b, 4H, -CH₂^d), 4.28-4.52 (m, 12H, -CH₂^{6+g+c}), 5.16-5.21 (m, 4H, -CH₂⁸), 5.83-5.98 (m, 4H, Ar-H^e), 6.30-6.51 (m, 4H, Ar-H^f), 6.92-7.52 (m, 36H, Ar-H^{9+10+11+a+a'+b}), 7.98 (m, 2H, Ar-H⁷), 8.18-8.28 (m, 2H, - Ar-H²⁺³), 8.67-9.07 (b, 4H, Ar-H¹ and -NH⁴). ¹³C-NMR (CDCl₃, 300 MHz, 298 K) δ (ppm) = 21.5 (3C, -aliphatic, -CH₃), 46.2- 47.7 (4C, aliphatic, -NHCH₂CH₂NH-, peak corresponds to wheel component), 49.5 (2C, aliphatic, peak corresponds to the carbon where H₆, H_g or H_c is attached), 58.8 - 59.2 (2C, aliphatic, peak corresponds to axle component where H₈ is attached), 65.3 (2C, aliphatic, aliphatic carbon in which any one of H_d, H₅ is attached), 67.7- 68.0 (2C, any one of the aliphatic carbon where either H₆, H_g, or H_c is attached), 108.0 (Ar-C, corresponds to the carbon where any one of H_a, H_{a'}, H_b is attached), 113.1-113.8 (4C, Ar-C, corresponds to the carbon where H_e is attached), 120.8 (Ar-C), 124.2-124.6 (Ar-C), 125.1-130.1 (Ar-C), 135.8-136.1 (Ar-C), 142.3-142.7 (Ar-C), 147.9-148.6 (Ar-C), 155.8-156.9 (Ar-C), 165.6-165.7 (Ar-C), 178.1 (C=O). Anal. Calculated for C₁₀₀H₉₅N₁₃O₁₃: C, 71.20; H, 5.68; N, 10.79, found: C, 71.42; H, 5.58, N, 10.88.

(l) Synthesis of rotaxane, ROTb:

[2]rotaxane, ROT' (186 mg, 0.1 mmol, 1.0 eqv.) was dissolved in dry CH₂Cl₂ in a 50 mL R.B. flask and 4.0 equivalent of trifluoro acetic acid (0.076 mL, 10.0 eqv.) is added in the reaction mixture. Then the reaction mixture was allowed to stir at room temperature for 12h. The solvent along with the acids was evaporated to obtain a sticky mass which mainly contains protonated rotaxanes with trifluoro acetate counter anions. The crude product was used in the next step without further isolation and purification. To the sticky mass in the 50 mL R.B. dry CH₂Cl₂ was added. Then triethyl amine (0.70 mL, 5.0 eqv. with respect to the trifluoro acetic acid) was added as a base. After stirring for 10 min at room temperature, 3.5 equivalent 4-fluorobenzoyl chloride (0.05 mL, 0.4 mmol, 0.4 eqv) was added in the reaction mixture and was allowed to stir at room temperature for another 6h. Then the reaction mixture was poured into a 100 mL separating funnel and washed with plenty of water, saturated sodium bicarbonate solution and brine solution for 2-3 times respectively. The organic phase was evaporated under reduced pressure to obtain tris aryl ring appended functionalized rotaxane, ROTb as a white powder. Yield 152 mg (79%) M.P. above 200° C. ESI-MS (+ve mode): m/z calcd. for C₁₁₅H₉₈N₁₃F₃O₁₃Na [M+Na]⁺, 1949.7290, found 1949.7250. FTIR in KBr disc (v/cm⁻¹): 3423, 3062, 2323, 2852, 1731, 1647, 1618, 1595, 1531, 1512, 1465, 1434, 1348, 1294, 1220, 1178, 1049, 1006, 854, 759, 702. ¹H-NMR in CDCl₃ (500 MHz, 298K) (mixture of rotamers), δ (ppm) = 3.30 (b, 8H, -CH₂^{h+i}), 3.65 - 4.02 (m, -CH₂^{c+d+g+5+6}), 5.23 (m, 4H, -CH₂⁸), 6.07-6.22 (s, 4H, Ar-H^e), 6.51-6.80 (m, 4H,

Ar-H^f), 7.05-7.47 (m, 50H, Ar-H^{9+10+11+a+a'+b+7+1+m}), 7.74 (b, 2H, Ar-H³), 8.10-8.24 (m, 2H, -NH₄), 8.37 (b, 2H, Ar-H²), 8.85 (s, 2H, Ar-H¹). ¹H-NMR in DMSO-d₆ (300 MHz, 298K) (mixture of rotamers), δ (ppm) 3.31 (b, 8H, -CH₂^{h+i}), 3.52-3.77 (b, 8H, -CH₂^{c+d}), 4.42 (b, 8H, -CH₂^{6+c}), 4.62 (d, 4H, -CH₂^g), 5.16 (s, 4H, -CH₂⁸), 6.22 (s, 4H, Ar-H^e), 6.60 (b, 4H, Ar-H^f), 7.07-7.48 (m, 36H, Ar-H^{9+10+11+a/a'+b}), 8.05 (s, 2H, -Ar-H⁷), 8.28 (b, 2H, Ar-H³), 8.36 (b, 2H, Ar-H²), 8.75 (b, 2H, -NH₄), 8.91 (s, 2H, Ar-H¹). ¹³C-NMR (CDCl₃, 300 MHz, 298 K) δ (ppm) = 28.6 (4C, aliphatic, -NHCH₂CH₂NH-), 50.3 (2C, aliphatic), 53.5 (2C, aliphatic), 55.4 (2C, aliphatic), 67.3 (2C, aliphatic), 78.3 (2C, aliphatic), 78.5, 79.7 (2C, aliphatic), 79.7 [total 9 types of aliphatic carbon], 108.7, 115.9, 121.1, 127.6, 128.4, 130.4, 136.9, 142.9, 149.1, 157.0, 165.4, 172.7, 177.5 (3C, C=O).). Anal. Calculated for C₁₁₉H₁₁₀F₃N₁₃O₁₃:C, 71.92; H, 5.58; N, 9.17, found: C, 71.47; H, 5.78, N, 8.99.

(m) Synthesis of acetylated rotaxane, ROTc:

A similar procedure was followed to obtain crude protonated MC based rotaxane with trifluoro acetate counter anions as applied for ROTb synthesis. To the sticky mass obtained in 50 mL R.B. was dissolved in dry CH₂Cl₂ and triethyl amine (0.70 mL, 5.0 eqv. with respect to the trifluoro acetic acid) was added as a base. After stirring it for 10 min at room temperature, 3.5 equivalent distilled pivaloyl chloride (0.05 mL, 0.4 mmol, 0.4 equivalent) was added in the reaction mixture and was allowed to stir at room temperature for additional 5h. Then the reaction mixture was poured into a 100 mL separating funnel and water was added, then the biphasic layer was shaken well for 2-3 times. After that, a saturated solution of sodium bicarbonate and brine solution was used for washing for 2-3 times respectively. The organic phase was evaporated under reduced pressure to obtain three tertiary butyl group appended functionalized rotaxane, ROTc as a white powder. Yield 265 mg (81%). M.P. above 200° C. ESI-MS (+ve mode): m/z calcd. for C₁₀₉H₁₁₄N₁₃O₁₃[M+H]⁺, 1836.8590, found 1836.8563. ¹H-NMR in CDCl₃ (500 MHz, 298K) (mixture of rotamers), δ (ppm) 1.27-1.40 (m, 9H, -C(O)(CH₃)₃), 1.75 (b, 8H, -CH₂^{h+i}), 3.46-3.64 (m, 8H, -CH₂^{c+d}), 3.83 (m, 4H, -CH₂⁶), 4.36 (m, 4H, -CH₂⁵), 4.68 (b, 4H, -CH₂^g), 5.24 (s, 4H, -CH₂⁸), 6.08 (s, 4H, Ar-H^e), 6.72 (b, 4H, Ar-H^f), 7.17-7.47 (m, 36H, Ar-H^{9+10+11+a+a'+b+7}), 7.68 (b, 2H, Ar-H³), 8.22 (b, 2H, -NH₄), 8.33 (d, 2H, Ar-H², J = 9 Hz), 8.83 (s, 2H, Ar-H¹). ¹H-NMR in DMSO-d₆ (300 MHz, 298K) (mixture of rotamers), δ (ppm)) 1.23 (m, 9H, -C(O)(CH₃)₃), 3.47 (b, 8H, -CH₂^{h+i}), 3.71-3.79 (m, 8H, -CH₂^{c+d}), 4.32 (d, 4H, -CH₂^{6+c}), 4.56 (d, 4H, -CH₂^g), 5.13 (s, 4H, -CH₂⁸), 6.08 (s, 4H, Ar-H^e), 6.62 (b, 4H, Ar-H^f), 7.05-7.44 (m, 36H, Ar-H^{9+10+11+a/a'+b}), 7.76 (b, 2H, Ar-H^{a'/a}), 8.02 (s, 2H, -Ar-H⁷), 8.21 (b, 2H, Ar-H³), 8.32 (d, 2H, Ar-H², J = 9 Hz), 8.71 (b, 2H, -NH₄), 8.88 (s, 2H, Ar-H¹).). ¹³C-NMR (DMSO-d₆, 300 MHz, 298 K) δ (ppm) = 31.3-31.7, 45.9, 59.1, 67.4, 67.7, 68.1, 108.7, 115.8, 121.1, 124.7, 125.7, 126.9, 127.5, 128.3, 128.4, 129.6, 130.1, 130.6, 134.0, 141.8, 143.1, 146.4, 149.1, 152.6, 157.0, 158.5, 162.2, 165.5, 166.1, 173.0, 177.5, 182.6. Anal.

Calculated for $C_{113}H_{125}N_{13}O_{13}$: C, 72.45; H, 6.73; N, 9.72, found: C, 72.64; H, 6.66, N, 9.68. FTIR in KBr disc (ν/cm^{-1}): 3413, 3058, 2921, 2852, 1730, 1662, 1625, 1614, 1598, 1510, 1483, 1411, 1367, 1294, 1242, 1176, 1114, 1083, 952, 842, 750, 702, 638.

The rotation of the tertiary amide bonds (C=O)-NR₂ is expected to be in the range of the room temperature NMR time scale and has been observed at NMR experiments. The existence of such rotations generates the fluxional nature and forms conformers/ co-conformers of the interlocked molecules. Most importantly, not all of these conformers/ co-conformers are identical with respect to energy. In the NMR spectrum, along with the major signals, the very tiny signals are correspond to the protons which are actually representing the less populated isomers. Some of the signals of one conformers/ co-conformers may superimpose with each other/ or with other NMR-signals to some extent and thus, the evaluation is very difficult. At high temperature when all the amide rotations are fast, the signals for each conformers/ co-conformers become averaged. As the macrocycle is symmetrical and one of the amide groups (the middle one) is on the symmetry plane, we would therefore expect two sets of signals, one is for the two terminals -R groups, and the other one is for the middle R group. These facts are observed in case of ROTa (Figure 61S, SI at around 2.0-2.2 ppm region) and ROTb (Figure 5C, ¹⁹F-NMR spectrum in the main text).

However, we are pretty successful to evaluate the ¹H-NMR signals of the interlocked compounds (ROTa-c) by variable temperature ¹H-NMR experiments, ROESY, NOESY and COSY spectra analysis. We have tried to carried out high temperature ¹³C-NMR spectrum but our attempts was unsuccessful due to the (i) low solubility of the compound in DMSO-d₆ (as large amount is required to record ¹³C-NMR) and (ii) requirement of higher number of scan at high temperature compared to the ¹H-NMR spectrum. Thus, we are unable to assign properly the ¹³C-NMR spectra.

Associated Contents: Spectral Data such as NMR, Electronic spectra are provided in Supporting Information (ESI[†]). Saikat Santra: ORCID: <https://orcid.org/0000-0002-4198-3192>

Acknowledgements: PG is thankful to the Science and Engineering Research Board (SERB), New Delhi (project SR/S1/IC-39/2012) for financial support. S. Santra acknowledges the Council of Scientific & Industrial Research (CSIR) and IACS for fellowship. S.S. is thankful to Dhruvaa Halder for PL data recording.

References:

- (1) M. J. Langton and P. D. Beer, *Acc. Chem. Res.* 2014, **47**, 1935.
- (2) J. Y. C. Lim, I. Marques, V. Felix and P. D. Beer, *Angew. Chem. Int. Ed.* 2017, 220.

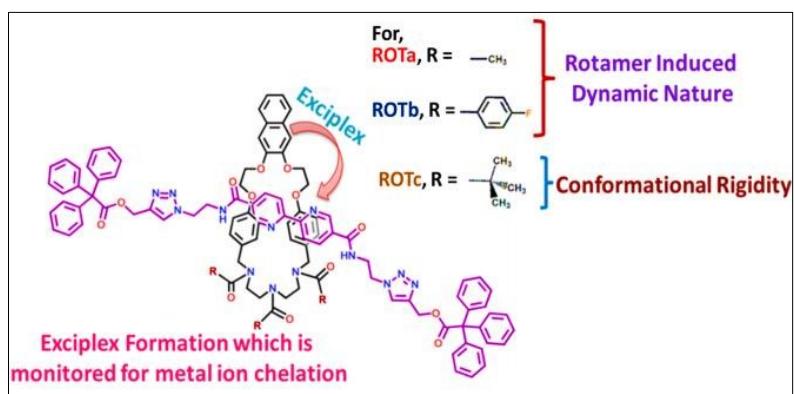
- (3) J. Y. C. Lim, I. Marques, A. L. Thompson, K. E. Christensen, V. Felix and P. D. Beer, *J. Am. Chem. Soc.*, 2017, **139**, 3122.
- (4) D. A. Leigh, V. Marcos and M. R. Wilson, *ACS Catal.* 2014, 4, 12, 4490.
- (5) J. Echavarren, M. A. Y. Gall, A. Haertsch, D. A. Leigh, V. Marcos and D. J. Tetlow, *Chem. Sci.*, 2019, **10**, 7269.
- (6) (a) J. Y. C. Lim and P. D. Beer, *Eur. J. Org. Chem.* 2019, **21**, 3433; (b) N. H. Evans, *Eur. J. Org. Chem.* 2019, **21**, 3320.
- (7) M. Dumartin, M. C. Lipke, J. F. Stoddart, *J. Am. Chem. Soc.* 2019, **141**, 18308.
- (8) D. Li, B. D. Smith, *J. Org. Chem.*, 2019, **84**, 2808.
- (9) R. Hein, P. D. Beer and J. J. Davis, *Chem. Rev.* *Chem. Rev.*, 2020, **120**, 1888.
- (10) (a) J. Y. C. Lim, I. Marques, V. Félix and P. D. Beer, *J. Am. Chem. Soc.*, 2017, **35**, 1222; (b) M. Inouye, A. Yoshizawa, M. Shibata, Y. Yonenaga, K. Fujimoto, T. Sakata, S. Matsumoto and M. Shiro, *Org. Lett.*, 2016, **18**, 1960, (c) Q. -Hui Guo, J. Zhou, H. Mao, Y. Qiu, M. T. Nguyen, Y. Feng, J. Liang, D. Shen, P. Li, Z. Liu, M. R. Wasielewski and J. F. Stoddart, *J. Am. Chem. Soc.*, 2020, doi.org/10.1021/jacs.0c01114; (d) K. Yang, S. Chao, F. Zhang, Y. Pei and Z. Pei, *Chem. Commun.*, 2019, **55**, 13198.
- (11) V. Blanco, D. A. Leigh, U. Lewandowska, B. Lewandowski and V. Marcos, *J. Am. Chem. Soc.* 2014, **136**, 15775.
- (12) V. Blanco, A. Carlone, K. D. Haenni, D. A. Leigh and B. Lewandowski, *Angew. Chem. Int. Ed.* 2012, **51**, 5166.
- (13) C. S. Kwan, A. S. C. Chan and K. C. F. Leung, *Org. Lett.* 2016, **18**, 976.
- (14) A. Fernandez, J. Ferrando-Soria, E. M. Pineda, F. Tuna, I. J. Vitorica-Yrezabal, C. Knappke, J. Ujma, C. A. Muryn, G. A. Timco, P. E. Barran, A. Ardavan and R. E. P. Winpenny, *Nat. Commun.* 2016, **7**, 10240.
- (15) J. E. Green, J. W. Choi, A. Boukai, Y. Bunimovich, E. Johnston-Halperin, E. DeIonno, Y. Luo, B. A. Sheriff, K. Xu, Y. S. Shin, H. R. Tseng and J. F. Stoddart and J. R. Heath, *Nature*, 2007, **445**, 414.
- (16) J. P. Sauvage, *Angew. Chem. Int. Ed.*, 2017, **56**, 11080.
- (17) J. F. Stoddart, *Angew. Chem. Int. Ed.*, 2017, **56**, 11094.
- (18) B. L. Feringa, *Angew. Chem. Int. Ed.*, 2017, **56**, 11060.
- (19) N. R. Van and D. Castelvechi, *Nature*, 2016, **538**, 152.
- (20) S. Erbas-Cakmak,; D. A. Leigh, C. T. Mc. Ternan and A. L. Nussbaumer, *Chem. Rev.*, 2015, **115**, 10081.
- (21) T. R. Kelly, J. P. Sestelo and I. Tellitu, *J. Org. Chem.*, 1998, **63**, 3655.
- (22) T. Lang, E. Graf, N. Kyritsakas and M. W. Hosseini, *Dalton Trans.*, 2011, **40**, 5244.

- (23) I. N. Meshkov, V. Bulach, Y. G. Gorbunova, N. Kyritsakas, M. S. Grigoriev, A. Y. Tsivadze and M. W. Hosseini, *Inorg. Chem.*, 2016, **55**, 10774.
- (24) L. L. Pleux, E. Kapatsina, J. Hildesheim, D. Haeussinger and M. Mayor, *Eur. J. Org. Chem.*, 2017, **2017**, 3165.
- (25) C. Yu, L. Ma, J. He, J. Xiang, X. Deng, Y. Wang, X. Chen and H. Jiang, *J. Am. Chem. Soc.* 2016, **138**, 15849.
- (26) G. Wang, H. Xiao, J. He, J. Xiang, Y. Wang, X. Chen, Y. Che and H. Jiang, *J. Org. Chem.*, 2016, **81**, 3364.
- (27) M. Nakamura, K. Kishimoto, Y. Kobori, T. Abe, K. Yoza and K. Kobayashi, *J. Am. Chem. Soc.*, 2016, **138**, 12564.
- (28) J. Clayden and J. H. Pink, *Angew. Chem. Int. Ed.*, 1998, **37**, 1937.
- (29) P. Commins and M. A. G. Garcia-Garibay, *J. Org. Chem.* 2014, **79**, 1611.
- (30) J. E. Nunez, A. Natarajan, S. I. Khan and M. A. Garcia-Garibay, *Org. Lett.*, 2007, **9**, 3559.
- (31) R. Ait-Haddou and W. Herzog, *Cell Biochem. Biophys.*, 2003, **38**, 191.
- (32) D. A. Leigh, U. Lewandowska, B. Lewandowski and M. R. Wilson, *Top. Curr. Chem.*, 2014, **354**, 111.
- (33) K. Hirose, Y. Shiba, K. Ishibashi, Y. Doi and Y. Tobe, *Chem. Eur. J.*, 2008, **14**, 3427.
- (34) V. V. Bermudez, N. Capron, T. Gase, F. G. Gatti, F. Kajzar, D. A. Leigh, F. Zerbetto, S. Zhang, *Nature*, 2000, **406**, 608.
- (35) H. A. Wegner, *Angew. Chem. Int. Ed.*, 2012, **51**, 2281.
- (36) N. Fuentes, A. Martin-Lasanta, L. Alvarez de Cienfuegos, M. Ribagorda, A. Parra and J. M. Cuerva, *Nanoscale*, 2011, **3**, 4003.
- (37) I. Arahamian, *Nat. Chem.*, 2016, **8**, 97.
- (38) I. Arahamian, *Chem. Commun.*, 2017, **53**, 6674.
- (39) P. R. Ashton, R. Ballardini, V. Balzani, S. E. Boyd, A. Credi, M. T. Gandolfi, M. Gomez-Lopez, S. Iqbal, D. Philp, J. A. Preece, L. Prodi, H. G. Ricketts, J. F. Stoddart, M. S. Tolley, M. Venturi, A. J. P. White and D. J. Williams, *Chem. Eur. J.*, 1997, **3**, 152.
- (40) L. Ma, S. Wang, C. Li, D. Cao, T. Li and X. Ma, *Chem. Commun.*, 2018, **54**, 2405.
- (41) G. Ragazzon, A. Credi and B. Colasson, *Chem. Eur. J.*, 2017, **23**, 2149.
- (42) S. J. Rao, Q. Zhang, J. Mei, X. H. Ye, C. Gao, Q. C. Wang, D. H. Qu and H. Tian, *Chem. Sci.*, 2017, **8**, 6777.
- (43) M. Sutesh, A. K. Mandal, E. Suresh and A. Das, *Chem. Sci.*, 2013, **4**, 4532.
- (44) M. Gangopadhyay, A. Maity, A. Dey, P. R. Rajamohanan, S. Ravindranathan and A. Das, *Chem. Eur. J.* 2017, **23**, 18303.

- (45) S. Saha, S. Santra and P. Ghosh, *Org. Lett.* 2015, **17**, 1854.
- (46) V. Balzani, A. Credi and M. Venturi, *Chem. Soc. Rev.*, 2009, **38**, 1542.
- (47) P. Stacko, J. C. M. Kistemaker, T. van Leeuwen, M. C. Chang, E. Otten and B. L. Feringa, *Science*, 2017, **356**, 964.
- (48). (a) J. E. M. Lewis, M. Galli and S. M. Goldup, *Chem. Commun.*, 2017, **53**, 298; (b) M. J. Mac Lachlan, A. Rose and T. M. Swager, *J. Am. Chem. Soc.*, 2001, **123**, 9180; (c) M. Gangopadhyay, A. Maity, A. Dey, P. R. Rajamohanam, S. Ravindranathan, A. Das, *Chem. Euro. J.* 2017, **23**, 18303; (d) S. Kushwaha, A. Maity, M. Gangopadhyay, S. Ravindranathan, P. R. Rajamohanam and A. Das, *Langmuir*, 2017, **33**, 10989; (e) M. Gangopadhyay, A. Maity, A. Dey and A. Das, *J. Org. Chem.*, 2016, **81**, 8977; (f) A. Maity, M. Gangopadhyay, A. Basu, S. Aute, S. S. Babu and A. Das, *J. Am. Chem. Soc.* 2016, **138**, 11113; (g) M. Gangopadhyay, A. K. Mandal, A. Maity, S. Ravindranathan, P. R. Rajamohanam and A. Das, *J. Org. Chem.*, 2016, **81**, 512; (h) A. K. Mandal, M. Gangopadhyay and A. Das, *Chem. Soc. Rev.*, 2015, **44**, 663; (i) A. K. Mandal, M. Suresh, M. K. Kesharwani, M. Gangopadhyay, M. Agrawal, V. P. Boricha, B. Ganguly and A. Das, *J. Org. Chem.* 2013, **78**, 9004; (j) A. K. Mandal, P. Das, P. Mahato, S. Acharya and A. Das, *J. Org. Chem.*, 2012, **77**, 6789.
- (49) J. S. Laursen, J. Engel-Andreasen, P. Fristrup, P. Harris and C. A. Olsen, *J. Am. Chem. Soc.*, 2013, **135**, 2835.
- (50) R. A. Bragg, J. Clayden, G. A. Morris and J. H. Pink, *Chem. Eur. J.*, 2002, **8**, 1279.
- (51) H. Tian and Q. C. Wang, *Chem. Soc. Rev.* 2006, **35**, 361.
- (52) C. J. Bruns and J. F. Stoddart, *Acc. Chem. Res.*, 2014, **47**, 2186.
- (53) G. Gholami, K. Zhu, G. Baggi, E. Schott, X. Zarate and S. J. Loeb, *Chem. Sci.*, 2017, **8**, 7718.
- (54) B. Riss-Yaw, C. Clavel, P. Laurent and F. Coutrot, *Chem. Commun.* 2017, **53**, 10874.
- (55) (a) W. Clegg, C. G. -Saiz, D. A. Leigh, A. Murphy, A. M. Z. Slawin and S. J. Teat, *J. Am. Chem. Soc.* 1999, **121**, 4124; (b) Y. Okuma, T. Tsukamoto, T. Inagaki, S. Miyagawa, M. Kimura, M. Naito, H. Takaya, T. Kawasaki and Y. Tokunaga, *Org. Chem. Front.*, 2019, **6**, 1002; (c) T. Nakamura, Y. Mori, M. Naito, Y. Okuma, S. Miyagawa, H. Takaya, T. Kawasaki and Yuji Tokunaga, *Org. Chem. Front.*, 2020, **7**, 513.
- (56) J. E. M. Lewis, P. D. Beer, S. J. Loeb and S. M. Goldup, *Chem. Soc. Rev.* 2017, **46**, 2577.
- (57) G. Baggi, S. J. Loeb, *Chem. Eur. J.*, 2017, **23**, 14163.
- (58) S. Prusty, S. Krishnaswamy, S. Bandi, B. Chandrika, J. Luo, J. S. Mc-Indoe, G. S. Hanan and D. K. Chand, *Chem. Eur. J.*, 2015, **21**, 15174.
- (59) M. Nandi, S. Santra, B. Akhuli and P. Ghosh, *Dalton Trans.* 2017, **46**, 7421.
- (60) S. Saha, S. Santra and P. Ghosh, *Eur. J. Inorg. Chem.*, 2014, **2014**, 2012.
- (61) W. Zhou, J. Li, X. He, C. Li, J. Lv, Y. Li, S. Wang, H. Liu, D. Zhu, *Chem. Eur. J.* **2008**, **14**, 754.

- (62) S. Saha, I. Ravikumar, P. Ghosh, *Chem. Eur. J.*, 2011, **17**, 13712.
- (63) M. Denis, L. Qin, P. Turner, K. A. Jolliffe and S. M. Goldup, *Angew. Chem., Int. Ed.* **2018**, **57**, 5315
- (64) M. Denis, J. Pancholi, K. Jobe, M. Watkinson, S. M. Goldup, *Angew. Chem. Int. Ed.*, 2018, **57**, 5310.
- (65) P. Ghosh, P. K. Bharadwaj, S. Mandal and S. Ghosh, *J. Am. Chem. Soc.*, 1996, **118**, 1553.
- (66) P. Ghosh, P. K. Bharadwaj, J. Roy and S. Ghosh, *J. Am. Chem. Soc.*, 1997, **119**, 11903.
- (67) S. Santra, P. Ghosh, *Eur. J. Org. Chem.*, 2017, **2017**, 1583.
- (68) S. Santra, S. Bej, M. Nandi, P. Mondal and P. Ghosh, *Dalton Trans.*, 2017, **46**, 13300.
- (69) E. Ishow, A. Credi, V. Balzani, F. Spadola, L. Mandolini, *Chem. Eur. J.*, 1999, **5**, 984.
- (70) K. Hiratani, M. Kaneyama, Y. Nagawa, E. Koyama and M. Kanosato, *J. Am. Chem. Soc.*, 2004, **126**, 13568.
- (71) (a) X. Ma and H. Tian, *Chem. Soc. Rev.*, 2010, **39**, 70; (b) J. Shi, Y. Xu, X. Wang, L. Zhang, J. Zhu, T. Pang and X. Bao, *Org. Biomol. Chem.*, 2015, **13**, 7517; (c) K. M. Mullen, J. J. Davis and P. D. Beer, *New J. Chem.*, 2009, **33**, 769; (d) E. Arunkumar, P. K. Sudeep, P. V. Kamat, B. C. Noll and B. D. Smith, *New J. Chem.*, 2007, **31**, 677.
- (72) S. Munding, U. Jakob, P. Bichovski, W. Bannwarth, *J. Org. Chem.*, 2012, **77**, 8968.
- (73) A. L. Bartuschat, K. Wicht and M. R. Heinrich, *Angew. Chem. Int. Ed.*, 2015, **54**, 10294.
- (74) S. Santra, S. Mukherjee, S. Bej, S. Saha and P. Ghosh, *Dalton Trans.*, 2015, **44**, 15198.
- (75) S. Saha, S. Santra, B. Akhuli and P. Ghosh, *J. Org. Chem.*, 2014, **79**, 11170.

T.O.C.



Fluorophoric [2]rotaxanes form exciplex upon interpenetration and the exciplex signals are used to monitor the chelation properties of interlocked systems